İSTANBUL TEKNİK ÜNİVERSİTESİ ⋆ FEN BİLİMLERİ ENSTİTÜSÜ

GEZEGENLERARASI MANYETİK ALAN VE İYONOSFERSEL KRİTİK FREKANSLAR ÜZERİNDEKİ OLASI ETKİLERİ

YÜKSEK LİSANS TEZİ

Müh. Orhan GÖKÇÖL

Ana Bilim Dalı : UZAY BİLİMLERİ VE TEKNOLOJİSİ

Programı : UZAY

ŞUBAT 1991

ISTANBUL TECHNICAL UNIVERSITY ⋆ INSTITUTE OF SCIENCE AND TECHNOLOGY

INTERPLANETARY MAGNETIC FIELD AND ITS POSSIBLE EFFECTS ON THE IONOSPHERIC CRITICAL FREQUENCIES

M.Sc. THESIS

Orhan GÖKÇÖL , B.Sc.

Date of Submission : 21 January 1991

Date of Approval : 8 February 1991

Supervisor : Prof. Dr. Yurdanur TULUNAY

Member : Assoc. Prof. Dr. Gülçin KANDEMİR

Member : Assoc. Prof. Dr. C. Ruhi KAYKAYOĞLU

FEBRUARY 1991

ACKNOWLEDGEMENT

I wish to thank Prof. Dr. Yurdanur Tulunay for her encouragement and help throughout this work.

I also wish to thank Dr. Mike Hapgood (Rutherford Appleton Lab. UK) for providing the sample data, running my tediously long programs there and sending the results with some plots with patience.

Last but not the least, I wish to thank my family for their loving and permanent encouragement throughout my education.

CONTENTS

ABBREVATIONS:

A :	Away polarity of the IMF
amu :	Atomic mass unit
AU :	Astronomical Unit
B :	Magnetic field strength
B_X,B_Y,B_Z :	Interplanetary magnetic field components in the GSM coordinate system
ΔB_Z:	Change in B_Z during a reversal
D,E,F,$F1$,$F2$:	Regions of the earth's ionosphere
dip :	Dipole
e :	Electron, electronic charge
$\vec{E}$:	Electric Field
emf :	Electromotive Force
EUV :	Extremely Ultra Violet Radiation
f% :	Fraction defining how stable the IMF B_Z is
$foF2$:	Ionospheric Critical Frequency
$\overline{foF2}$:	Arithmetic average of the $foF2$
$\delta foF2$:	Ionospheric Critical Frequency (Diurnal variations removed)
$\overline{\delta foF2}$:	Arithmetic average of the $\delta foF2$
GMT :	Greenwich Mean Time
GSM :	Geocentric Solar Magnetospheric
h :	Planck's constant
h :	Hour
$h\nu$:	Photon energy
HF :	High Frequency
Hz :	Hertz (cycle per second)

i : Angle of incidence

IMF : Interplanetary Magnetic Field

K : Kelvin

kHz : Kilohertz

km : Kilometer

lat : Latitude

long : Longitude

m_e : Mass of an electron

MHz : Megahertz

n : Number density

n_o : Neutron

N_e : Electron number density

nPa : Nanopascal

NSSDC : National Space Science Data Center

nT : Nanotesla

p : Proton

P: Solar Wind dynamic pressure

ΔP: Change in P during a B_Z reversal

R : Cross correlation coefficient

R_{SSN} : International Sun Spot Number

R_E : Earth's Radius

rad : Radian

RAL : Rutherford Appleton Laboratory

s : Second

SSB : Solar Sector Boundary

SW : Solar Wind

T : Toward polarity of the IMF

US : United States

V : Velocity

V_e : Drift velocity

ω : Angular frequency

ω_p : Natural angular plasma frequency

WDC : World Data Center

ϵ_o : Dielectric constant of the empty space

μ_o : Magnetic permeability

ν : Frequency

ρ : Density

σ : Tensor conductivity

Φ : Electrostatic potential

SUMMARY

In this study, it was aimed to discover possible links between interplanetary magnetic field (IMF), magnetosphere and ionosphere by using the hourly IMF, solar wind (SW) and ionospheric critical frequency ($foF2$) data obtained from World Data Center (WDC), over a period of 24 years (1963 – 1986).

In order to analyse the IMF data, the data were sorted out in three components; B_X,B_Y,B_Z; by employing GSM cartesian coordinate system. Since the IMF B_Z component plays an essential role in the energy transfer from the SW to the magnetosphere, there was more emphasize on IMF B_Z during the data analysis. The results revealed that there were some systematic seasonal and diurnal variations with respect to the solar rotation axis in the IMF B_Z component. During the 12.2% of the data coverage the IMF B_Z was stable for more than 2 hours. This stability seemed to be controlled by the solar cycle variation. Also, there was a clear solar cycle effect on the intensity of the IMF, B. It was searched whether there was any possible link between B_Z reversals (termed as "event") and the SW dynamic pressure changes. It was found out that neither southward nor northward turnings of the IMF were accompanied by major dynamic pressure changes.

In the second part of this work the possible effects of the IMF configuration on the ionospheric critical frequency, $foF2$, were investigated by employing the Slough $foF2$ data. For this purpose, first, the regular diurnal variations in the Slough $foF2$ data were removed. The new set of data formed such was referred as $\delta foF2$. Although there was a clear solar cycle variation in the Slough $foF2$ data; there was not a similar behaviour observed in the Slough $\delta foF2$ data. The possible effects of the several configurations of the IMF on the $\delta foF2$ data were searched by expressing the percent variations of the $\delta foF2$ with respect to the control curve which consisted of the hourly means of the $\delta foF2$ of the whole data set covering the period between 1967 and 1986. Several configurations of the IMF included northward and southward turnings of the IMF B_Z along with the towards and the away polarities of the IMF B_X components. The results of the analysis showed that that during the events, generally, $\overline{\delta foF2\%}$ increased during dusk and night hours, and they exhibited an oscillatory behaviour. On the other hand, there seemed to be no clear solar cycle effect on the $\overline{\delta foF2\%}$ during the events. It was also shown that southward IMF turnings produced greater diurnal $\overline{\delta foF2\%}$ variations compared to those cases associated with the northward IMF. During the unsteady variations of the IMF B_X component (referred as the solar sector boundary crossings) the southward IMF turnings seemed to be more influential over the $\delta foF2$ than those changes of the IMF B_X reversals. On the other hand, in the case of a northward IMF B_Z turning, B_X reversals seemed to be more dominant over the Slough $\delta foF2$ values than the direction of the IMF B_Z turning.

ÖZET

GEZEGENLERARASI MANYETİK ALAN VE İYONOSFERSEL KRİTİK FREKANSLAR ÜZERİNDEKİ OLASI ETKİLERİ

GİRİŞ

Güneşin enerjisi güneşin içinde nükleer tepkimeler sonucunda üretilir. Bu enerji 2 grupta toplanabilir : Elektromanyetik enerji ve tanecik enerjisi. Fotonlar ($h\nu$) tarafından taşınan güneşin elektromanyetik enerjisi yerin yüksüz atmosferi ile etkileşir ve iyonosferi oluşturur. Çoğunlukla elektron, proton,nötron (e,p,n_o) ve iyonize olmuş atomlardan oluşan tanecik enerjisi ise yerin manyetik alanı ile etkileşir ve manyetosferi oluşturur. Genellikle "Güneş Rüzgarı" olarak adlandırılan tanecik yayılımı güneşten radyal doğrultuda ve sürekli olarak akar (Şekil 1.1). Bu sürekli akan güneş rüzgarının güneşin içindeki hidrodinamik genişlemenin bir sonucu olduğu görüşü oldukca yaygındır [1]. Güneş rüzgarının hızı ,dünyadan 1 Astronomik Birim uzaklıkta, yaklaşık olarak 300 kms^{-1} dir. Diğer bir değişle güneş rüzgarı güneşten radyal doğrultuda süpersonik hızlarda sürekli akan sıcak ($\approx 10^5 K^o$) bir plazmadır.

Güneş rüzgarının dinamik basıncı,$\rho V^2/2$, manyetik basıncından ,$B^2/2\mu_o$, büyük olduğu için plazma ,güneşten yayılıyorken, kendi manyetik alanını hapseder [1] (V:güneş rüzgarı hızı, B:manyetik alan şiddeti, μ_o:manyetik geçirgenlik). Bu hapsolmuş alan uzayda gezegenlerarası manyetik alanı oluşturur.

Gezegenlerarası manyetik alanın ana kaynağı olan güneşin manyetik alanı, uydu gözlemlerine göre, (dünyanın dönme düzlemi içinde) manyetik kutupluluğun ya güneşe doğru; ya da güneşten uzaklaşan yönde olmasına göre bazı az ya da çok düzenli bölgelere ayrılır [4,5]. Manyetik alan, bu bölgesel düzenliliği uzunca bir süre değişmeden korur (saatler, bazen de günlerce). Bir manyetik kutupluluktan diğerine geçiş ise dakikalar ya da saatler mertebesindedir [1]. Güneş kendi ekseni edrafında döndüğü için bu manyetik kutupluluk ta döner ve etkisi dünyaya kadar taşınır (Şekil 1.2).

Eğer dünya bütünüyle boşluk içinde olsaydı, manyetik alanı dış uzaya genişleyecek ve güneş ile diğer gezegenlerin manyetik alanları ile yavaşça birleşecekti. Ancak, gezegenlerarası ortam bir boşluk değildir ve dolayısıyla etkileşim çok daha karmaşıktır. Güneş rüzgarının toplam basıncı manyetik basınç ile parçacıkların momentumları dolayısıyla sahip oldukları kinetik basıncın toplamına eşittir [6]. Yerin manyetik alanının da bir basıncı vardır. Gezegenlerarası ortamın basıncı ile yerin manyetik alanının basıncı karşılaştırıldığında, dünyadan uzaklarda güneşin manyetik alanı yerin manyetik alan etkisini yok edecek; dünyanın yakınlarında ise yerin manyetik alanı tarafından güneşin manyetik alan etkisi önlenecektir [1,7]. Orta bir uzaklıkta her iki basınç değerinin karşılaştırılabileceği bir bölge mutlaka var olmalıdır. Bu bölge manyetik ara bölgesi (magnetopause) olarak adlandırılır. Sesüstü hızlarda hareket eden güneş rüzgarı bir engel ile –yerin manyetik alanı– karşılaştığında bir şok dalgası oluşur. Bu, eğik şok (bow shock) olarak adlandırılır (Şekil 1.3). Manyetik ara bölgesi dünyadan yaklaşık 10 yer yarıçapı; eğik şok ise 14 yer yarıçapı uzaklık- tadır [1]. Eğik şok ile manyetik ara bölgesi arasında kalan bölge manyetik kılıf (magnetosheath) olarak adlandırılır. Manyetik ara bölgesini de içine alan ve yerin manyetik alanının güneşin manyetik alanı tarafından hapsedildiği bölge ise manyetosfer olarak adlandırılır.

Manyetik ara bölgesinin konumu, güneş rüzgarının dinamik basıncındaki farklılıklar ile değişir [8]. Uydu gözlemlerine dayanan çalışmalara göre güneş rüzgarından manyetosfere olan enerji geçişi büyük ölçüde gezegenlerarası manyetik alan kuvvet çizgileri ile yerin manyetik alanının kuvvet çizgilerinin birleşmeleri ile olur [9]. Yüksek enlemlerde alan çizgileri gece tarafına doğru süpürülür ve uzunca bir manyetik kuyruk oluştururlar. Manyetik kuyruk, dünyanın arkasında 1000 yer yarıçapından da uzakta gözlenmiştir [2,3].

İyonosfer, serbest elektronların radyo dalgalarının yayılımını etkileyebilecek kadar çok olduğu, yer atmosferinin bir bölgesi olarak tanımlanır [10]. İyonosfer, elektron yoğunluğuna göre D, E ve F olarak adlandırılan tabakalara bölünür. F tabakası ise, $F1$ ve $F2$ şeklinde iki ayrı tabakaya daha bölünür (Şekil 1.4).

İyonosferdeki iyonizasyon, radyo haberleşmeciliğindeki rolünden dolayı çok önemlidir. İyonosferin gönderilen bir dalgaya etkisi 2 türlü olabilir: (i) yansıtma (ii) yutma. Bir dalganın yansıtılmasına neden olan elektronlar yüksek (F tabakası); yutulmasına neden olan elektronlar ise düşük (D tabakası) bölgelerdedir [7] (Şekil 1.5). İyonosfersel plazma

$$\omega_p = \sqrt{\frac{N_e e^2}{\epsilon_o m_e}} \quad rad/s \tag{1}$$

doğal plazma frekansında titreşir [11]. Burada, N_e elektron yoğunluğu; e elektron yükü; m_e elektron kütlesi; ϵ_o ise boş uzaya ait dielektrik sabitidir. Bir elektromanyetik dalga, eğer frekansı doğal plazma frekansından büyükse, iyonosferi delebilir; aksi durumlarda dalga iyonosfer tarafından yansıtılacaktır. Bir başka değişle kritik frekans olarak ta adlandırılan, dik açıda gönderilen ve iyonosferde yansıtılan en büyük radyo dalgası frekansı, ω_c

$$\omega_c = \sqrt{80.6 N_{max}} \quad rad/s \tag{2}$$

olarak ifade edilir [11].

$F2$ tabakasına ait kritik frekans, $foF2$, dik açıda yerden gönderilen bir radyo dalgasının yansıdığı yükseklikteki maksimum elektron dağılımının bir ölçüsüdür. Bu şekilde tanımlanan kritik frekans, iyonosfersel olaylar için oldukça önemli bir parametredir [12]. Haberleşme amaçları için bir radyo dalgası, yansıtılabilmesi ve uzak mesafelerde alınabilmesi için, oldukça büyük bir gelme açısına sahip olmalıdır. Eğer i gelme açısı ise (2) denklemi,

$$\omega_c = \sqrt{\frac{80.6 N_{max}}{cos^2 i}} \quad rad/s \tag{3}$$

şeklini alır. Kritik frekans, i nin 90 dereceden düşük değerleri için artacaktır.

İyonosferde, elektron yoğunluğunun zamanla değişimi bir süreklilik denklemi ile ifade edilebilir [10].

[Elektron yoğunluğundaki değişim hızı] = [Üretim kazancı]
− [Kayıplar] ± [İletim dolayısıyla olan değişim] (4)

İyonosferin $200km$ altında, fotokimyasal olaylar önemlidir. $200km$ nin üzerinde ise dinamik olaylar önemlidir. Önemli dinamik olaylar şunlardır: $\vec{E} \times \vec{B}$ sapmaları (drift), yüksüz rüzgarlar, atmosferin genleşme ve büzülmesi ve elektron yayılmasıdır. Dinamik olaylar $F2$ tabakasının davranışında oldukça önemlidir. $\vec{E} \times \vec{B}$ sapmalarını bunlar içindeki önemi büyüktür.

Atmosferik hareketler havayı $\vec{V}$ hızı ile yerin manyetik alan çizgileri ötesine taşırlar. Alan çizgilerinin taşınması bir elektromotiv kuvvetin, $\vec{E}$, oluşmasına sebep olur. $\vec{E}$ aynı zamanda dinamo elektrik alanı olarak ta adlandırılır. Bu indüklenmiş alan, $\vec{E} = \vec{V} \times \vec{B}$, ortamın yüksüzlüğünü bozan bir akıma, $\sigma(\vec{V} \times \vec{B})$, sebep olur ($\sigma$,tansörel iletkenlik) ; dolayısıyla ters kutuplara sahip yükler (+ ve −) oluşur. Bu kutuplulaşma sonucu oluşan elektrostatik alan,$-\Delta\Phi$, nedeni ile ortam tekrar yüksüz hale gelir. Oluşan bu akımlar, çoğunlukla, E bölgesindedirler ve yerin manyetik alanında değişikliklere neden olurlar [13]. Oluşan elektrostatik alan, manyetik alan çizgileri yüksek derecede iletken oldukları için, F bölgesine iletilir ve burada $\vec{V}_e = (\vec{E} \times \vec{B})/B^2$ hızı ile verilen elektromanyetik sapmalara (electromagnetic drift) neden olur. Dolayısıyla, $\vec{E}$ ye zıt yönde bir dinamo elektrik alanı üretilir. Bu ise sapma hızlarını düşürür. Benzer şekilde, eğer manyetosferde dış etkenler sonucunda, $\vec{B}$ ye normal doğrultuda herhangi bir hareket olursa bu, F tabakasında iyon ve elektron hareketlerine neden olacaktır [14].

Yüklü parçacıkların iyonosferdeki davranışları büyük ölçüde yerin manyetik alanı tarafından kontrol edilir. Pek çok plazma gözlemlerinden çıkan sonuç, güneş rüzgarı ile yerin manyetik alanının etkileşiminin elektrik alanlar ürettiği şeklindedir [15]. Gözlemler, elektromanyetik sapmaların, gezegenlerarası manyetik alanın güney–kuzey bileşeninin,B_Z, güneye döndüğü durumlarda daha hızlı olmaya eğilimli olduğunu; B_Z nin kuzeye döndüğü durumlarda ise çok karmaşık bir yapıda bulunduğunu göstermiştir.

SONUÇLAR

Bu çalışmada, yukarıdaki paragraflarda açıklanmaya çalışılan, gezegenlerarası manyetik alan, manyetosfer ve iyonosfer arasındaki olası ilişkiler; Dünya Veri Bankası'ndan sağlanan 1963–1986 yılları arasındaki saatlik Gezegenlerarası Manyetik Alan ve Güneş Rüzgarı verileri ile 1967–1986 yılları arasında Slough (İngiltere, enlem:51.48, boylam:54.03) yer istasyonunda ölçülen iyonosferin $F2$ tabakasına ait saatlik kritik frekans, $foF2$, verileri kullanılarak araştırılmıştır. Gezegenlerarası manyetik alan verileri üç bileşeninin; B_X,B_Y,B_Z; davranışına göre incelenmiştir. Man- yetik alanın X,Y ve Z bileşenleri; başlangıç noktası yer merkezi olan, X ekseninin dünya güneş doğrultusunda, Z ekseninin X ekseni ile yerin dipol ekseninin bulunduğu düzlemde, Y ekseninin ise Z ekseninin bulunduğu düzleme dik doğrultudaki düzlemde bulunduğu bir kartezyen koordinat sisteminde ölçülen değerlerdir. (Şekil 2.1)

Gezegenlerarası manyetik alanın B_Z bileşeni güneş rüzgarından manyetosfere olan enerji geçişinde büyük rol oynadığı için [10] bu çalışmada ilk önce B_Z bileşeninin davranışı araştırılmıştır. Bu bileşenin, gezegenlerarası manyetik alanın kutupluluğuna göre mevsimlik ve günlük bazı sistematik davranışlar gösterdiği görülmüştür.$B_X < 0$ durumlarında, yılın ilk altı ayı için aylık ortalama B_Z değerleri sıfırdan büyük; ikinci altı ay için ise sıfırdan küçüktür. $B_X > 0$ durumlarında ise ilkine göre tam simetrik bir durum gözlenmiştir (Şekil 3.1). B_Z nin saatlik ortalama değişiminin ise aylık değişime göre daha küçük genliklere sahip olduğu görülmüştür.

Şiddeti ($|B_Z|$) $1nT$ dan büyük B_Z bileşenlerinden işaretini 1 saat içinde değiştiren B_Z durumları tespit edilmiştir. Bu durumlardan %12.2 sinde işaret değişikliğinden sonra B_Z bileşeninin işaretini 2 saatten daha fazla bir süre değiştirmediği görülmüştür. Bunlar, kararlı durumlar olarak adlandırılmıştır. Kararlı durumların yüzdesi küçük olduğu için iyonosfer-manyetosfer sistemi nadiren kararlı davranacaktır. Diğer bir değişle, B_Z işaretini fazla koruyamamaktadır. Dolayısıyla, B_Z deki değişimlerin oluşum zamanı iyonosferin yanıt zamanından daha düşük (veya karşılaştırılabilecek mertebelerde) olduğu için yer sisteminin genelde kararsız davrandığı söylenebilir.

Gezegenlerarası manyetik alanın B_Z bileşeninin işaretini değiştirdiği durumlarda güneş rüzgarı dinamik basıncındaki değişiklikler hesaplanmış ve bu değişimlerin dinamik basınçta büyük çapta değişiklikler oluşturmadığı görülmüştür (Şekil 3.5)

Slough kritik frekans değerleri ile güneş lekeleri arasında yüksek bir ilişki bulunmuştur. Ancak, aynı ilişki, $foF2$ verisinden günlük değişimler çıkarılarak (Ek A) elde edilen $\delta foF2$ verisinde gözlenememiştir (Şekil 3.6).

Gezegenlerarası manyetik alan yapısının iyonosfersel kritik frekanslar üzerindeki etkisi, yukarıda açıklanan B_Z değişimleri etrafında 8 saatlik $\delta foF2$ verileri alınarak araştırılmıştır. $\delta foF2$ yerine, tüm veriye ait $\delta foF2$ değerlerinin saatlik ortalaması alınarak oluşturulan bir kontrol eğrisine (Şekil 3.7) göre $\delta foF2$ nun % değişiminin kullanılması tercih edilmiştir. Bu analizden, gezegenlerarası manyetik alanın kuzey–güney bileşeninin iyonosfersel kritik frekanslar üzerinde bir kontrol oluşturduğu görülmüştür. Manyetik alanın güneye doğru yönlendiği durumlar kuzeye doğru olan durumlara göre daha büyük saatlik $\delta foF2$ % değerlerine sebep olmuştur. Ayrıca, güney yönündeki B_Z her saatte kontrol eğrisinden daha büyük $\delta foF2$ değerler indükliyorken, kuzey yönündeki B_Z geçişleri kontrol eğrisinden daha küçük değerler indüklemiştir (Şekil 3.10).

Bunun yanısıra, kuzeyden güneye olan gezegenlerarası manyetik alan geçişlerinde manyetik alanın x bileşeninin de (B_X) kritik frekans üzerinde bir kontrolü olduğu görülmüştür. Ancak bu durum, güney-kuzey gezegenlerarası manyetik alan geçişleri durumunda diğeri kadar belirgin değildir (Şekil 3.11).

Gezegenlerarası manyetik alan B_X bileşeninin kararsız davranışları sırasında (bir manyetik kutupluluktan diğerine geçiş) güneye yönelmiş B_Z bileşeninin kritik frekans değişimi üzerinde belirleyici rol oynadığı görülmüştür. Diğer yandan, kuzeye yönelmiş manyetik alan durumunda ise, B_Z bileşeninden çok manyetik kutupluluğun geçiş yönünün kritik frekanslar üzerinde etkili olduğu anlaşılmıştır (Şekil 3.12)

CHAPTER 1

INTRODUCTION

1.1. Solar Wind and its Interaction with the Geomagnetic Field

The sun's energy is generated in the solar core by means of nuclear reactions. This energy may be grouped into two components : electromagnetic energy and corpuscular energy. The solar electromagnetic energy that photons ($h\nu$) carry, interacts with the earth's neutral atmosphere and produces the ionosphere. The corpuscular energy which consists of mainly protons, electrons and neutrons (p, e, n_o) and ionised atoms interacts with the earth's magnetic field and produces the magnetosphere. Corpuscular radiation is often called the solar wind (SW) and it streams radially away from the sun continuously (Fig. 1.1). It is generally believed that the streaming SW is the result of a hydrodynamic expansion of the solar corona [1]. SW assumes a speed about 300 kms^{-1} at a distance of 1 Astronomical Unit (AU). In other words, the SW is a hot ($\approx 10^5 K^o$) supersonic plasma streaming radially from the solar corona [2,3].

Since the dynamic pressure, $\rho V^2/2$, of the SW is greater than the magnetic pressure, $B^2/2\mu_o$, the plasma imprisons its magnetic field [1] as it emerges from the sun (V is the SW speed, B is the magnetic field strength, μ_o is the magnetic permeability). This field forms the interplanetary magnetic field (IMF) in the space.

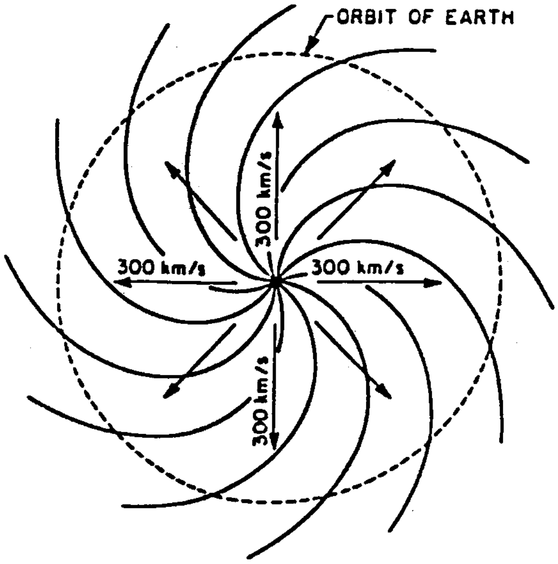

Figure 1.1 : The configuration of the interplanetary magnetic field in the equatorial plane for a steady state solar wind [1].

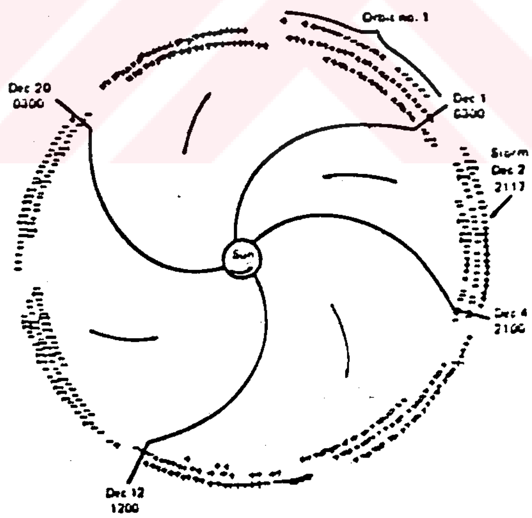

Figure 1.2 : Solar magnetic sector structure as inferred from IMP spacecraft observations. Plus signs (away from the sun) and minus signs (toward the sun) are 3–hourly measurments of IMF direction, and arrows in four sectors indicate predominant direction of the field [5]. (Note: unlike the convention adopted in this work, Wilcox adopted plus sign for an away polarity and minus sign for a toward polarity in this illustration.)

Based on the satellite observations, the solar magnetic field (which is the main source of the IMF) is divided into more or less regular sectors (in the earth's orbital plane) in which the magnetic polarity directed either toward (T polarity) or away (A polarity) from the sun, and any type of polarity remains constant for several days at a time [4,5]. Transitions from one sector to another take place over a period of minutes or hours [1]. The field polarity is apparently connected to the sun, and as the sun rotates, the field also rotates so that the sectors and the boundaries sweep past the earth (Fig. 1.2).

If the earth were in a perfect vacuum, its dipole field would extend outward, merging smoothly with the magnetic fields of the sun and the other planets. However, the interplanetary space is not a vacuum, it is filled with the SW in such a way that the interaction between the geomagnetic field and the SW becomes more complex. The total pressure of the SW is the sum of the pressure exerted by the momentum of the particles and the magnetic pressure [6], $B^2/2\mu_o$. The geomagnetic field also has a pressure. When the pressures of the interplanetary medium and the geomagnetic field are compared it is clear that at greater distances the geomagnetic field will be swept away by the SW and that close the earth the SW will be excluded by the geomagnetic field [1,7]. At intermediate distances, there must exist a region of interaction where the pressures are comparable. This boundary is called the magnetopause. Also, when the SW, or some hot plasma which is moving at supersonic speeds, encounters an obstacle, the geomagnetic field, a shock wave is formed. It is called the bow shock (Fig. 1.3). The magnetopause is at about $10R_E$ and the bow shock is at about $14R_E$ on the sun-earth line [1]. The region between them is called the magnetosheath. The region interior to the magnetopause is known as the magnetosphere. In other words, the magnetosphere is the region where the geomagnetic field is confined.

The location of the dayside magnetopause is known to be altered by the SW dynamic pressure changes. The SW, because of its dynamic pressure, compresses the magnetosphere [8]. Studies based on the spacecraft observations show that the supply of the SW energy into the magnetosphere proceeds mainly by reconnection between the lines of force of the IMF and the geomagnetic field [9]. The field lines from the high latitude regions are swept back toward the night side and form a long geomagnetic tail. The tail has been observed at a distance of more than $1000R_E$ behind the earth [1].

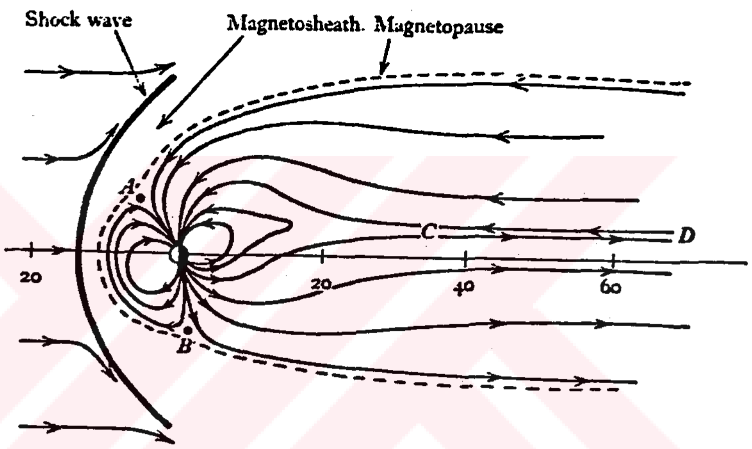

Figure 1.3 : The geomagnetic field lines distorted by the action of the solar wind. (Geocentric distances are in units of earth radii) [1].

1.2. The Coupling Between the Ionosphere and the Magnetosphere

The ionosphere is defined as the part of the earth's atmosphere in which free electrons are sufficiently numerous to influence the propogation of radio waves [10]. The ionosphere is divided into three characteristic layers named D, E, and F according to the electron concentration. The F layer is also subdivided into two other layers, $F1$ and $F2$ (Fig. 1.4).

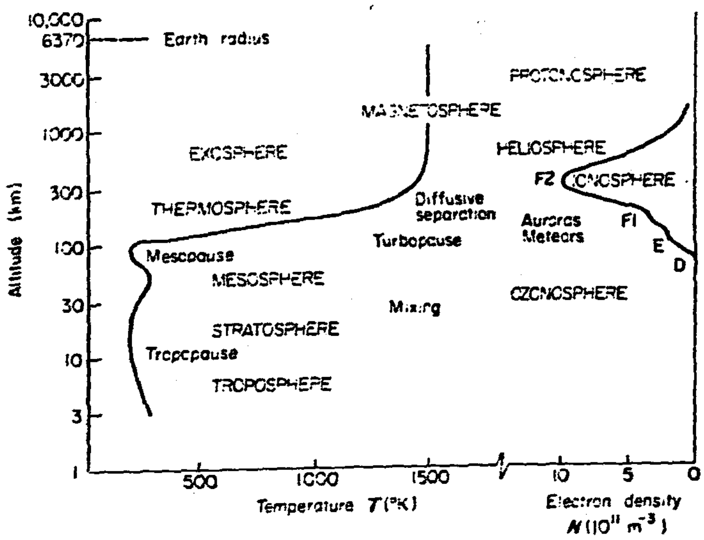

Figure 1.4 : Regions of atmosphere, showing conventional names describing levels, physical regimes, and characteristic constituents [10].

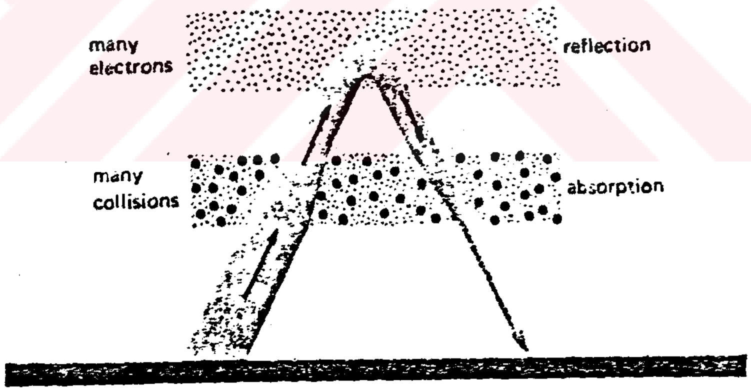

Figure 1.5 : Reflection and absorbtion of a wave in the ionosphere [7].

The ionisation in the ionosphere is of practical importance because of its role in radio communication. The ionosphere can do two different things to a wave : (i) reflection, (ii) absorption. The electrons responsible for the reflection are at greater heights (in the F layer), and those responsible for the absorbtion are lower down [7], in the D region where the collision frequency between the charged ions and the neutral species is greater than the corresponding gyro frequency (Fig. 1.5). The ionospheric plasma oscillates at the natural plasma frequency [11]

$$\omega_p = \sqrt{\frac{N_e e^2}{\epsilon_o m_e}} \quad rad/s \tag{1.1}$$

where N_e is the electron number density, e is the electronic charge, m_e is the mass of an electron and ϵ_o is the dielectric constant of the empty space. An electromagnetic wave may only propagate through the ionosphere provided that its propagation frequency ω is greater than ω_p ; otherwise the wave will be reflected. In other words, the highest radio frequency which is also called the critical frequency, ω_c that a layer will reflect at vertical incidence is [11]

$$\omega_c = \sqrt{80.6 N_{max}} \quad rad/s \tag{1.2}$$

where N_{max} is the maximum electron number density or concentration.

The critical frequency $foF2$ of the $F2$ layer (or the greatest frequency yielding reflection from the $F2$ layer of an upward-going radio signal at vertical incidence) is a measure of the maximum electron concentration at those altitudes. It may be considered as the single most significant characteristic parameter which is indicative of an ionospheric state [12]. For communication purposes over long distances, the radio signal must have a relatively large angle of incidence in order for the reflection from the ionosphere to be received at considerably long distances. If i is the angle of incidence of the transmitted radio wave the equation (1.2) takes the form [11]

$$\omega_c = \sqrt{\frac{80.6 N_{max}}{cos^2 i}} \quad rad/s \tag{1.3}$$

The critical frequency is increased when i is less than 90° providing N_{max} remains constant.

In the ionosphere, the time variation of the electron density can be expressed in terms of a continuity equation [10], which is

$$\text{[Rate of change of electron concentration]} = \text{[Gain by production]} - \text{[Loss by destruction]} \pm \text{[Change due to transport]} \quad (1.4)$$

In the ionosphere below 200 km the photochemical processes are important, whereas above 200 km the transport or the dynamical processes are dominant. The important dynamical processes are the ambipolar diffusion, $\vec{E} \times \vec{B}$ drifts, neutral winds, expansion and contraction of the atmosphere [10]. Since the dynamical processes exert considerable control on the behaviour of the F2 region it is instructive to summarize very briefly what an $\vec{E} \times \vec{B}$ drift is.

The atmospheric movements move the air with a velocity $\vec{V}$ across the geomagnetic field lines causing an electromotive force ,$\vec{E}$, to be set up. $\vec{E}$ is also called the "dynamo electric field". This induced field , $\vec{E} = \vec{V} \times \vec{B}$ drives a current $\sigma(\vec{V} \times \vec{B})$ which disturbs the charge neutrality of the medium (σ is the tensor conductivity), therefore, polarisation charges are set up. An electrostatic field, $-\Delta\Phi$, is set up which adjusts itself towards the charge neutrality again. These currents flow principally in the E region and cause the quiet variations in the geomagnetic field [13]. The electrostatic field associated with these charges is transmitted to the F region, since the magnetic field lines are highly conducting, where they cause electromagnetic drifts given by $\vec{V}e = (\vec{E} \times \vec{B})/B^2$. This motion in turn, generates a dynamo field that is opposed to $\vec{E}$, and therefore reduces the drift velocity of the particles. Conversly, if any motion of ionisation normal to $\vec{B}$ is set up in the magnetosphere by external causes, it will produce corresponding motions of the F region ions and electrons [14].

The behaviour of charged particles (ions and electrons) in the ionosphere (especially in the E and F region) is largely governed by the earth's magnetic field. From many observations of plasma motions, it is known that the interaction between the SW, as it sweeps past the earth, and the geomagnetic field sets up a systems of electric fields [15]. Observations show that the drift tends to be faster at times when the south – to north B_Z component of the IMF is directed southward and has got a more complex pattern when B_Z is directed northward [10].

CHAPTER 2
DATA ANALYSIS

2.1. Introduction

Radio waves in the wide frequency range from Very Low Frequency (VLF) to High Frequency (HF) ($3\,kHz$ to $30\,MHz$) can be propagated to great distances via the ionosphere. The changes which occur in the height distribution of the ionospheric electron densities which exhibits day to day variability greatly affect the propagation characteristics of these waves [1,15].

In this work, the objective is to search the possible effects of the IMF configuration on the ionospheric critical frequencies. Since both the IMF B_Z turnings and magnetic sector structures seem to be responsible for dynamical variations of the upper atmosphere , such a possible influence of the IMF on the ionospheric critical frequencies may be plausible [10].

The data analysis were grouped in two parts. In the first part an extensive study was carried out only by taking the solar data into consideration. For this purpose a survey was done of hourly averages of observations of the IMF and the SW made by satellites at about 1 AU in the years between 1963 and 1986. Since the reversals of B_Z of the IMF cause significant changes in the magnetosphere in turn at the ionospheric altitudes [10], the present investigation was confined to major reversals of B_Z. Therefore, "events" were identified as times when there was a reversal of the polarity of B_Z between the adjacent hourly mean values. Then, a statistical analysis were conducted in terms of the three cartesian components of the IMF and the SW data.

The study of day-to day variability of ionospheric critical frequencies is of scientific interest in view of the causative mechanisms and of great importance in assessing prediction capabilities [16]. The variability in ionospheric critical frequencies, which is of practical importance in communication systems, navigational control applications [12], etc. can be studied for example by investigating the role of the IMF structure as an ordering parameter. If the direction of the IMF affects a special geophysical parameter its effect should be most marked during changeovers of the IMF polarity, the so-called IMF sector boundary crossings. Therefore, in recent years many activities have been done to investigate the influence of the IMF direction on geomagnetic activity [4,16,17,18]. In the second part of this investigation the Slough ionospheric critical frequencies were studied between 1967 and 1986. Since the task to cary out such an exercise was to see the possible influence of the IMF structure on the ionospheric critical frequencies some simple statistical methods were employed. To do this, first the diurnal variations were removed from the critical frequencies. Then they were analysed in detail for several definite IMF configuration for twenty years.

2.2. The Data

The data used in this work have been taken from a compilation of solar wind plasma and IMF data prepared by the US National Space Science Data Center

(NSSDC). The data were supplied by a number of experimental groups and they were recorded on a number of spacecraft close to the earth (i.e. 1 AU) : IMP-1, IMP-3 to -8, AIMP-1 and -2, OGO-5, HEOS, VELA-2 to -6, ISEE-1 to -3 [19]. The data were read off magnetic tape and stored on-line in a number of data bases which operated under a formal management system called R-EXEC. This system was developed at Rutherford Appleton Laboratory (RAL) for the manipulation of scientific data [20].

The coordinate system used for presenting magnetic field data is the geocentric solar magnetospheric (GSM) system -a right handed cartesian system with coordinates X_{sm}, Y_{sm}, Z_{sm}. The origin of the coordinate system is assumed at the center of the earth. The positive X_{sm} axis is directed toward the sun. Y_{sm} axis lies in the ecliptic plane and Z_{sm} axis lies in the plane containing both the X_{sm} axis and the geomagnetic dipole axis [1] (Fig. 2.1).

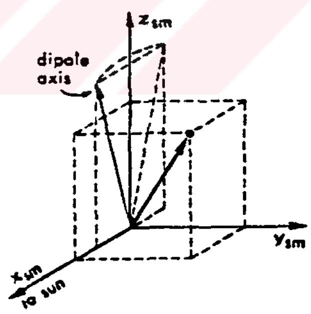

Figure 2.1 : Geocentric solar magnetospheric (GSM) coordinate system [1].

The data set available to this work covers a period from 2 November 1963 to 31 May 1987. There were two complete solar cycle, that is 20th and 21st, included in the analysis. Within this period, only the cases for which both plasma and magnetic field data are available simultaneously, were examined. This restricted the analysis to the period 27 November 1963 to 4 April 1986. Within this period there were 101558 hourly values available out of a total 195960 hours possible. This provides an average availability of 52 % of the data coverage.

The ionospheric critical frequency data, $foF2$, used here were taken from the World Data Center at the Rutherford Appleton Laboratory (WDC - RAL). The critical frequencies were obtained from the ground - based station, Slough, England (51.48 Geo. Lat.,-0.57 Geo. Long. ; 54.03 Dip. Lat., 84.44 Dip. Long.). By taking the hourly value of $foF2$ and substracting the quiet day control value of the $foF2$ for the same local time, the diurnal variations were eliminated. The new data set obtained such is going to be referred as $\delta foF2$ (App. A).

2.3. Definition of an "event"

A reversal of the polarity of the IMF B_Z component between hourly data points was named an "event" (with start time t_1 and finish time $t_2 = t_1 + 1$ hour) provided that $|B_Z| > 1\,nT$ for both data points. These events were, then, divided according to the behaviour of B_X and B_Y during the reversal of B_Z. Events with reversals of B_X or B_Y, both, neither or with absent data points, were binned for seperate statistical analysis.

2.4. Distribution of IMF, SW, $foF2$, $\delta foF2$ Values

In order to get accustomed to the IMF, SW, $foF2$ and $\delta foF2$ data the following histograms were constructed: Figure 2.2a shows the distribution of SW speed which ranged between 250 kms^{-1} and 950 kms^{-1} with a mode value of 370 kms^{-1} . Figure 2.2b shows the SW densities which ranged up to 83 cm^{-3} with a mode value of 6 cm^{-3} . The SW dynamic pressure as defined by [8] is $P = nmv^2$. Taking the mean mass of the SW, m, to be 1 a.m.u. (i.e. the SW is assumed to be predominantly protons and electrons), P is found to have ranged up to 28 nPa (Fig. 2.2c). Figure 2.3a shows that the magnitude of the IMF varies between 0 and 85 nT. The mode value is 6 nT. Figure 2.3b shows the distribution of B_Z values in GSM coordinates. The smallest and the largest B_Z values were $-31\,nT$ and $27\,nT$ respectively. The calculated mean value is 0.014 nT. The values of B_Z are normally distributed and northward and southward fields occur with equal frequencies. From this figure it is seen that the most probable B_Z value is less than 1 nT. This finding is in general agreement with the notation that a steady spherically expanding SW would have no B_Z component in the sun's equatorial plane [1]. Figure 2.4a shows the distribution of the $foF2$ values for Slough in the period of interest. The calculated mean, mode and median values of the $foF2$ are 5.712 MHz, 5.7 MHz, 5.0 MHz respectively. In Fig. 2.4b the distribution of $\delta foF2$ values were presented. The distribution is skewed towards negative $\delta foF2$ values. It is believed that the preference for more negativeness of the $\delta foF2$ may be due to [1] : only quiet days were used to derive the control curve. These would be the days of highest $foF2$ values as the effect of magnetic activity was to reduce $foF2$. Thus $\delta foF2$ would be biased towards the negative values.

In the second part of the analysis the critical frequencies obtained around an event time were considered mainly. In order to enrich the statistics, the events with IMF data available for at least three hour before and after an event (i.e. major IMF B_Z reversal) were preferred to use. In addition to this criteria the events further were selected only if the direction of the IMF B_Z kept its sign three hours before

[1]Private communications with Dr. Mike Hapgood, Rutherford Appleton Lab. England

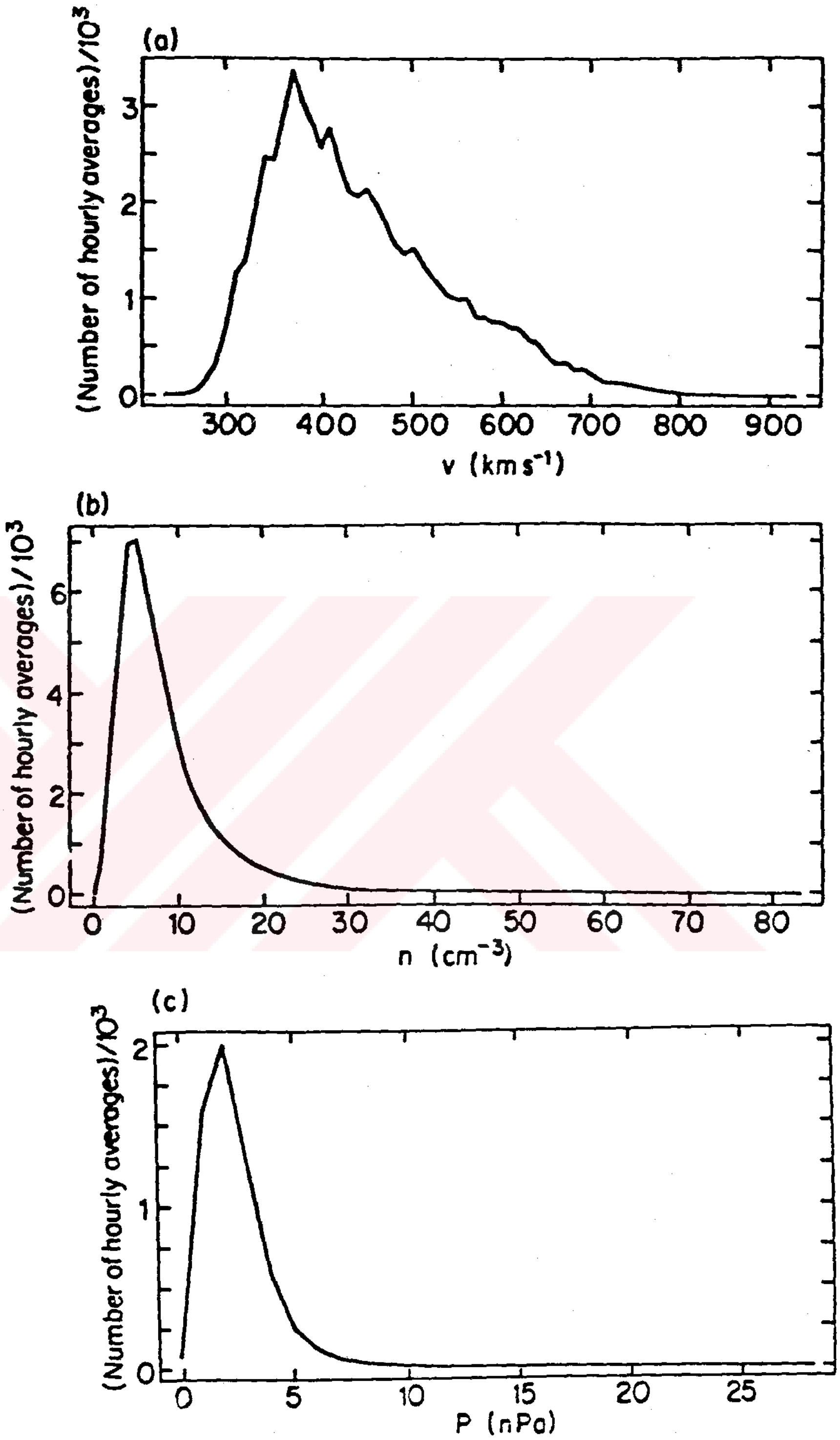

Figure 2.2 : The distribution of (a) the solar wind speed, V; (b) the solar wind density, n; (c) the solar wind dynamic pressure, P.

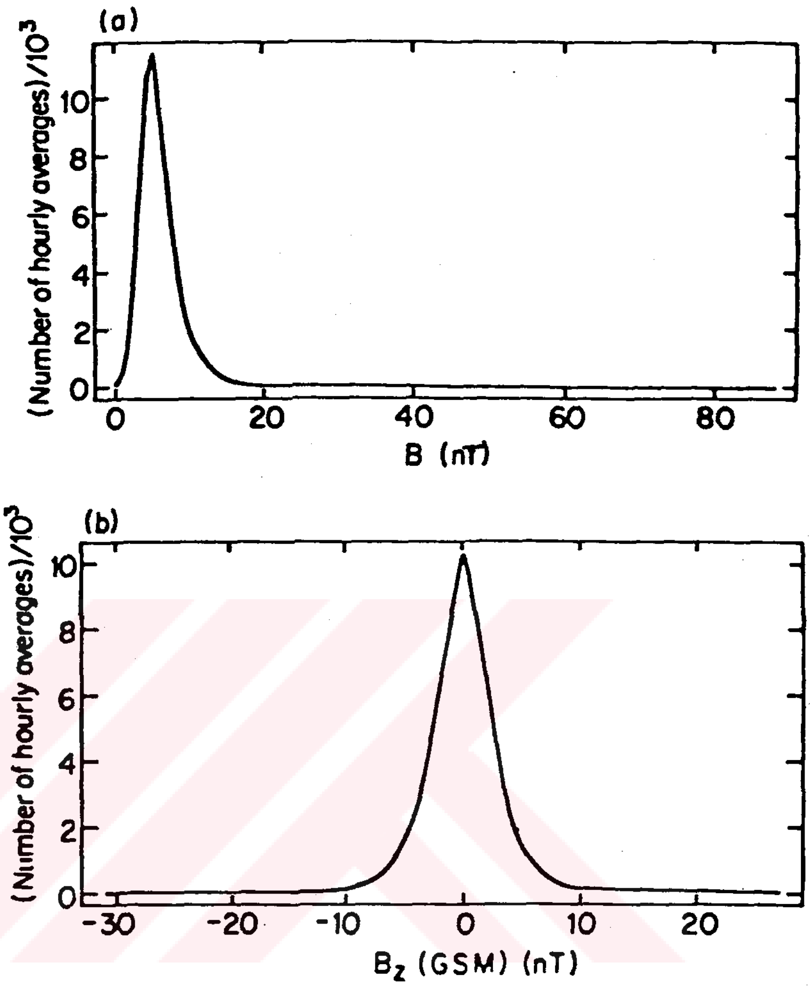

Figure 2.3 : The distribution of (a) the IMF strength, B; (b) the northward component of the IMF (in GSM coordinate system), B_Z.

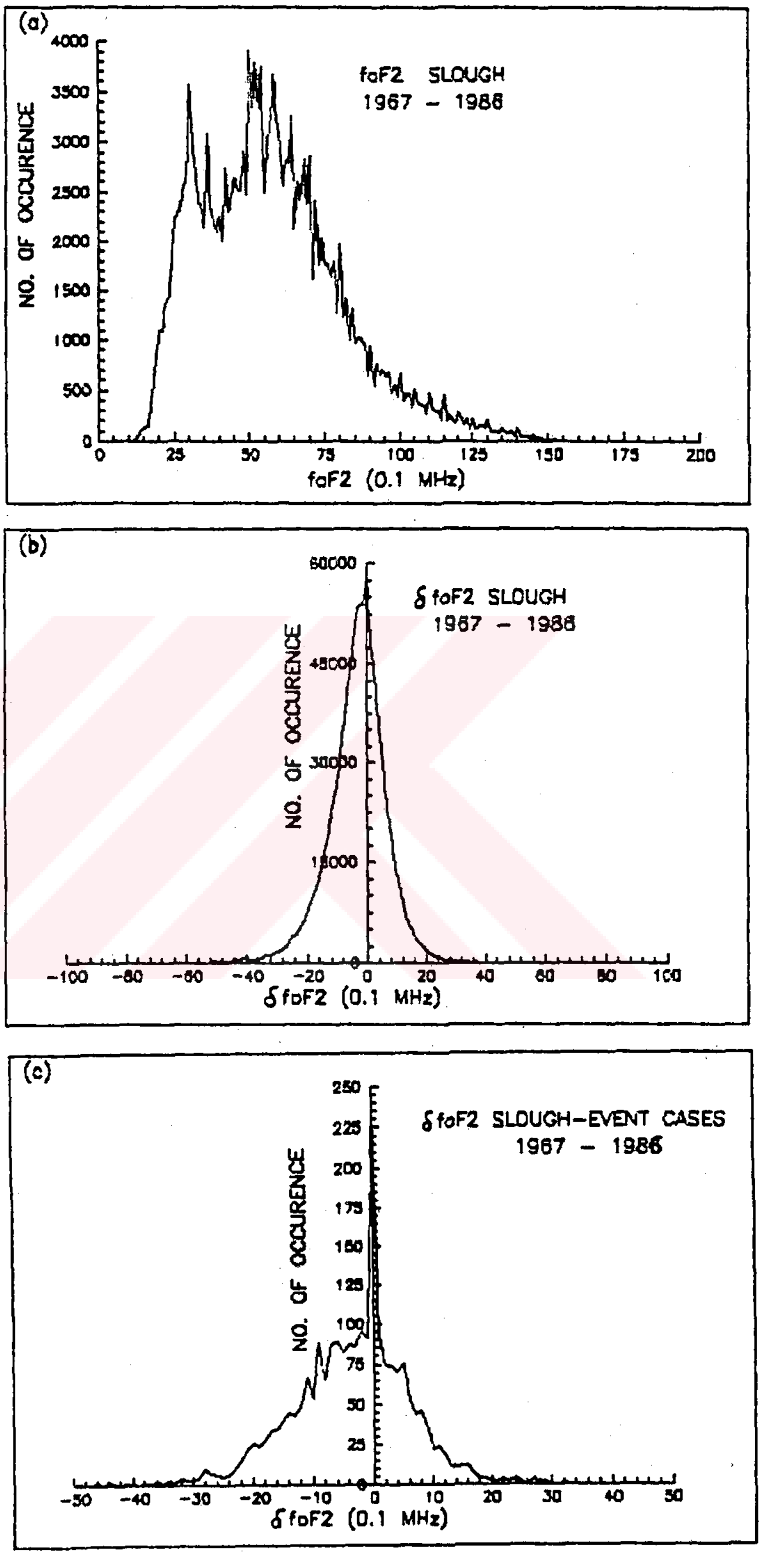

Figure 2.4 : The distribution of the Slough (a) $foF2$ values; (b) $\delta foF2$ values; (c) $\delta foF2$ values during IMF B_Z reversals.

and three hours after a B_Z reversal. In other words, there were no other events occured, as far as our data revealed, for eight hours during a specific event under consideration. Unless specified otherwise an "event" will imply such isolated cases detected within an eight hour interval of time. Fig. 2.4c shows the distribution of the $\delta foF2$ values chosen for eight hours for each of such event cases.

CHAPTER 3

RESULTS AND CONCLUSIONS

3.1. The Results on the Solar Wind and the Interplanetary Magnetic Field Between 1963 – 1986

3.1.1. Statistical Results for the Interplanetary Magnetic Field (IMF)

The interplanetary magnetic field data were analysed by a computer program (App. B). The program searched for events using the criteria given in Section 2.3. A total of 6018 events were found between 1967 and 1986. The results may be summarixed as follows:

1. About 49 % of the events were northward and 51 % of them were southward.
2. For 24 % of the events neither B_X nor B_Y reversals took place during a B_Z reversal.
3. For 24 % of the events either B_X or B_Y did not change for at least eight hours (from t_1 − 3h to t_2 + 3h).
4. For 9% of the events there were reversals of either B_X or B_Y during a B_Z reversal while the other component kept the same sign for at least eight hours

(from $t_1 - 3$h to $t_2 + 3$h).

5. For 9% of the events there were either B_X or B_Y reversals.

6. For 3% of the events there were reversals of both B_X and B_Y during a B_Z reversal.

7. For 31% of the events there were either too many B_X or B_Y reversals or there were data gaps between $t_1 - 3$h and $t_2 + 3$h giving no clear results.

The well defined events (2,4,6) have also been sorted by polarity of B_X and B_Y at time t_1:

- 17% had B_X positive and B_Y negative,
- 15% had B_X negative and B_Y positive,
- 2% had B_X positive and B_Y positive,
- 2% had B_X negative and B_Y negative.

From this analysis it can easily be seen that the probability of having the same sign for IMF B_X and B_Y is very low (2%). In other words during a B_Z reversal most of the time the horizontal IMF component of B_{XY} in the ecliptic plane is either in the second (06-12 GMT) or in the fourth (18-24 GMT) quadrant of the (X,Y) cartesian coordinate system. By considering either B_X or B_Y, the other component can be interpreted at least in sign. Unless stated otherwise from here on only the results of the data analysis based on the various configuration of IMF B_X and B_Z will be presented for the sake of the simplicity. It is assumed that one vertical component and one horizontal component are enough for the first part of the work in which the possible influence of the IMF on the ionospheric critical frequencies will be sought.

3.1.2. Mean Variations of the IMF B_Z Component for $B_X < 0$ and $B_X > 0$

The vertical component, B_Z, induced by the IMF in the geocentric solar magnetospheric (GSM) coordinate system plays an essential role in the energy transfer from the solar wind into the magnetosphere [4,9]. As stated with emphasize, the negative B_Z component should favour the energy transfer from the solar wind into the magnetosphere, on the other hand positive B_Z values should inhibit such an input [4]. Therefore, the B_Z values employed in this work were further analysed in order to understand better the diurnal and seasonal dependence of the IMF B_Z data.

The B_Z component is expected to show some systematic variations due to diurnal and seasonal changes of the earth's dipole axis with respect to the solar rotation axis. Figure 3.1a shows the results of an investigation of the seasonal and diurnal variations of the IMF B_Z component for $B_X < 0$ (defined as A polarity) and $B_X > 0$ (defined as T polarity) for the years 1982, 1983, 1984. From this figure it can be seen that an IMF with A polarity induced positive B_Z values during the spring half year (January to June), and negative B_Z values during the autumn half year (July to December). On the other hand an IMF with T polarity caused a symmetrical picture in B_Z variation. IMF sectors with negative B_Z values are called pro-sectors and IMF sectors with positive B_Z values are called anti-sectors [4]. In Fig. 3.1b the diurnal variation of the IMF B_Z component was presented. It can be seen that the diurnal B_Z variation had smaller amplitudes than those of the seasonal B_Z component.

Table 3.1. summarizes the results obtained in Fig. 3.1a,b. Figure 3.1a,b and Table 3.1. reveal that the seasonal variation of the IMF B_Z component has

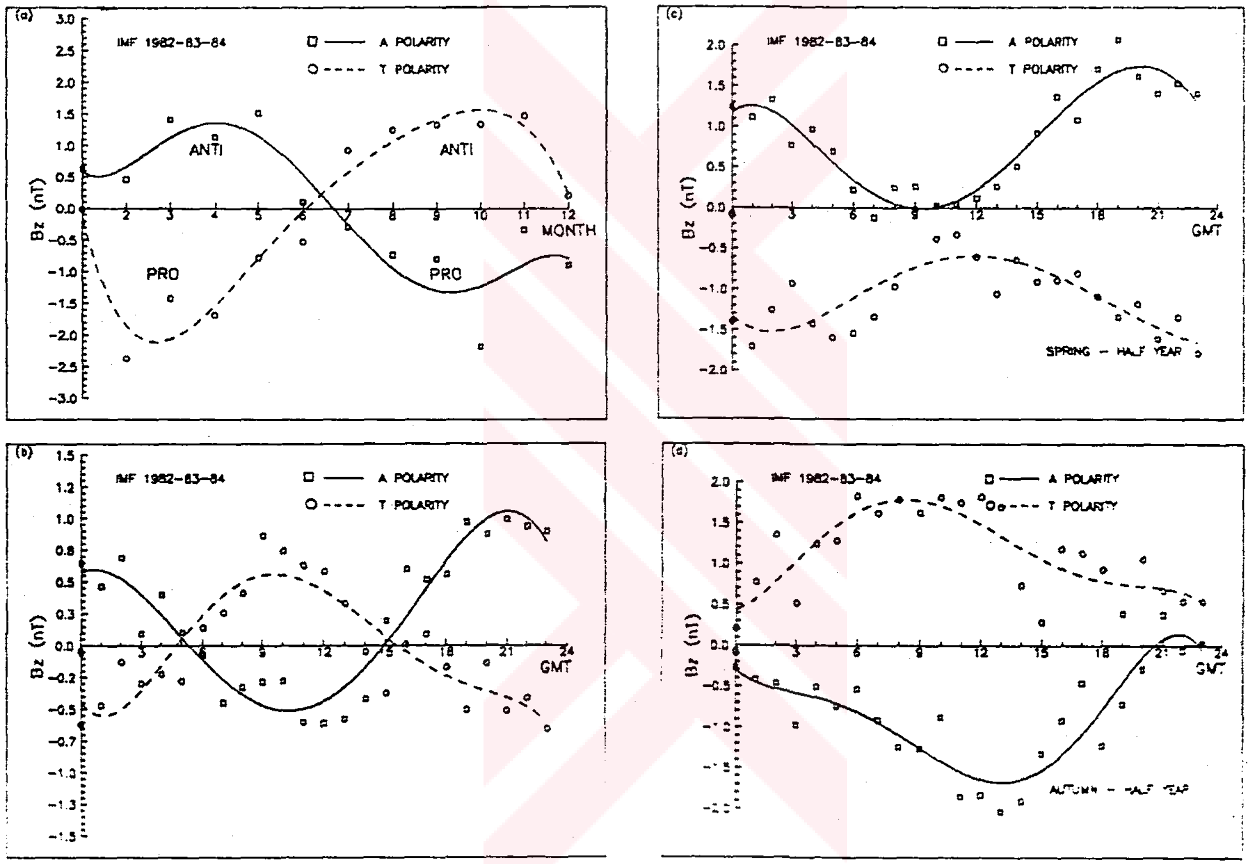

Figure 3.1 : Mean (a) seasonal; (b) diurnal; (c) spring–half diurnal; (d) autumn–half diurnal variations of the IMF B_Z component for A and T polarities. The best fit 5th degree orthogonal polynomials were drawn to illustrate the general trends in the data.

got minimum values (pro-sectors) near (20-24-2)GMT and in March for T polarity whereas the corresponding time and month are (9-10-11)GMT and September, October respectively. For the A polarity, on the other hand, IMF B_Z component has got maximum values (anti sectors) near (8,9,10)GMT and in September for T polarity whereas the corresponding time and month are (23-24-02)GMT and April respectively.

Table 3.1.

Seasonal and Diurnal Variations of the IMF B_Z Component (1982,83,84)

	T Polarity	A Polarity
PRO ($B_Z < 0$)	March, April (Min.) (20–24–02GMT)	Sept., Oct. (Min) (09–10–11GMT)
ANTI ($B_Z > 0$)	Sept.,Oct. (Max.) (08–09–10GMT)	April (Max.) (23–00–02GMT)

In order to remove the seasonal bias the B_Z data then seperated into two groups. The first group included the data for the months January to June, and the second group included the data for the months July to December of 1982,1983,1984. Figure 3.1c shows the diurnal variation of the IMF B_Z component for the Spring half year, and Fig. 3.1.d shows the results of the autumn half year. The data were, then, regrouped for Pro ($B_Z < 0$) and Anti ($B_Z > 0$) sectors in Fig. 3.2a and in Fig. 3.2b. Such a seperation of the data showed that the T polarity curve lagged approximately 12 hours behind the A polarity curve. This was an indication of solar control over the data under investigation. Summarizing, Fig. 3.2. exhibited the diurnal behaviour of the IMF B_Z. In this diurnal variation, both in the Anti and Pro sectors, the polarity of the solar sector structure played an important role.

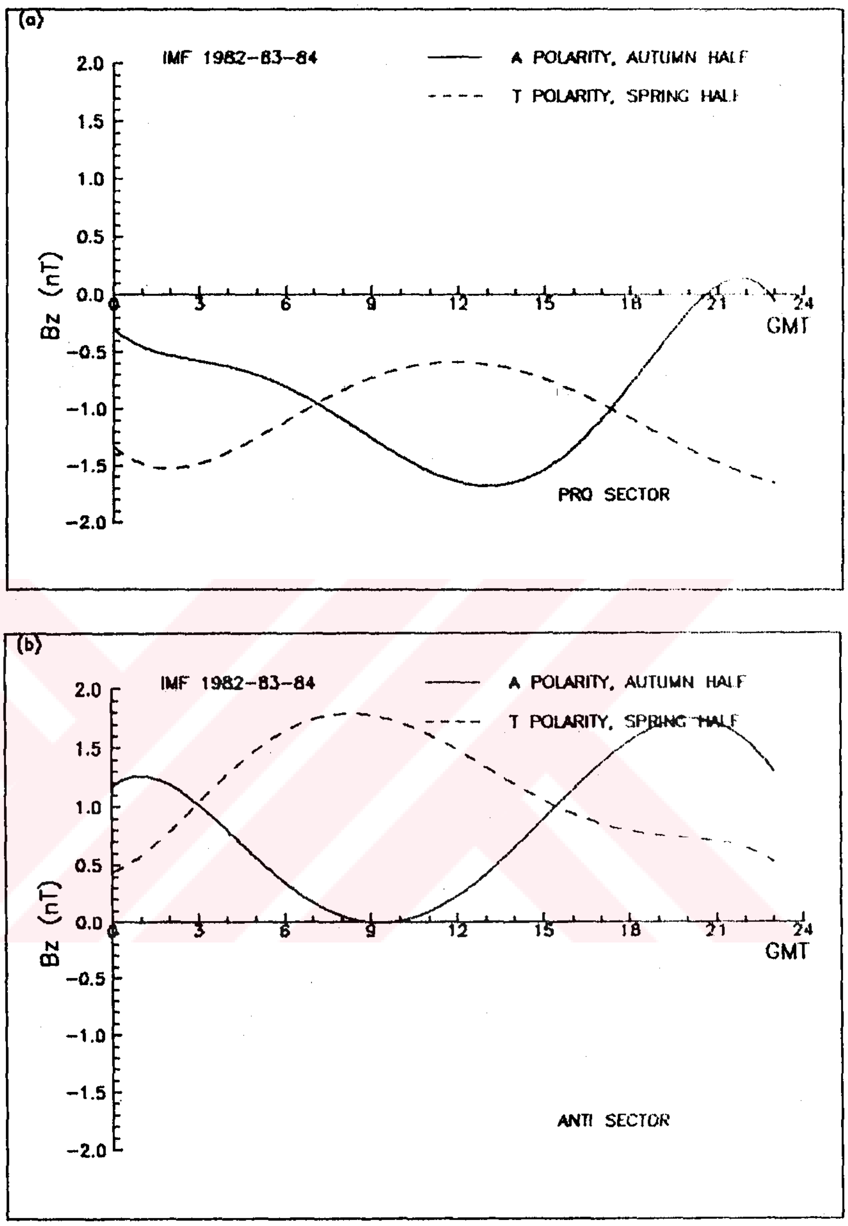

Figure 3.2 : Mean diurnal variations of the IMF B_Z component for (a) Pro ($B_Z < 0$); (b) Anti ($B_Z > 0$) sectors. The best fit 5th degree orthogonal polynomials are shown.

3.1.3. The Stability of IMF B_Z Component

To estimate the duration of stable IMF conditions, the period following each event for which B_Z maintained constant sign was determined. Cases in which data gaps occured before B_Z changed its sign were excluded from the analysis. Figure 3.3 shows the number of times that a particular period of stable B_Z sign occured in the data set for both B_Z reversals. The minimum period shown in the figure is 1 hour. Such cases indicate that the IMF B_Z changes its sign again immediately after an "event" and so B_Z has constant sign for only one hour. The two distributions (i.e. for northward and southward B_Z turnings) are almost identical as can easily be seen in the figure. It was, then, calculated the number of cases for which the sign of B_Z was stable for more than 2 hours. For the whole data set it was found that this number was 2007 out of a total of 5277 cases in which the period of stability could be measured. This amounts to 38% of all cases. The total duration of these periods is 12,369 hours, which is 12.2% of the total number of hours in the study.

To investigate the solar - cycle dependence of the stability of IMF B_Z component, the cases in which B_Z keeps its sign that of at t_2 (i.e. after a B_Z reversal which termed "event"), more than 3 hours for each year were carried out and compared with the international sunspot numbers. Figure 3.4a shows the event cases (upper panel) defined as a fraction ($f\%$) of total number in the years between 1963 – 1986 and Fig. 3.4b shows the international sunspot numbers (R_{SSN}) (lower panel) in the same year range. From these figures there seemed to be a solar – cycle variation in the stability of the IMF B_Z component. The cross correlation coefficient between R_{SSN} and $f\%$ was 0.53. At the significance level of $\alpha = 0.05$, this value is greater than the theoretical cross correlation coefficient of $R = 0.34$ indicating a possible positive influence of a solar cycle control. Since $f\%$ is a fraction which is proportional to the number of events in which B_Z keeps its sign more than three

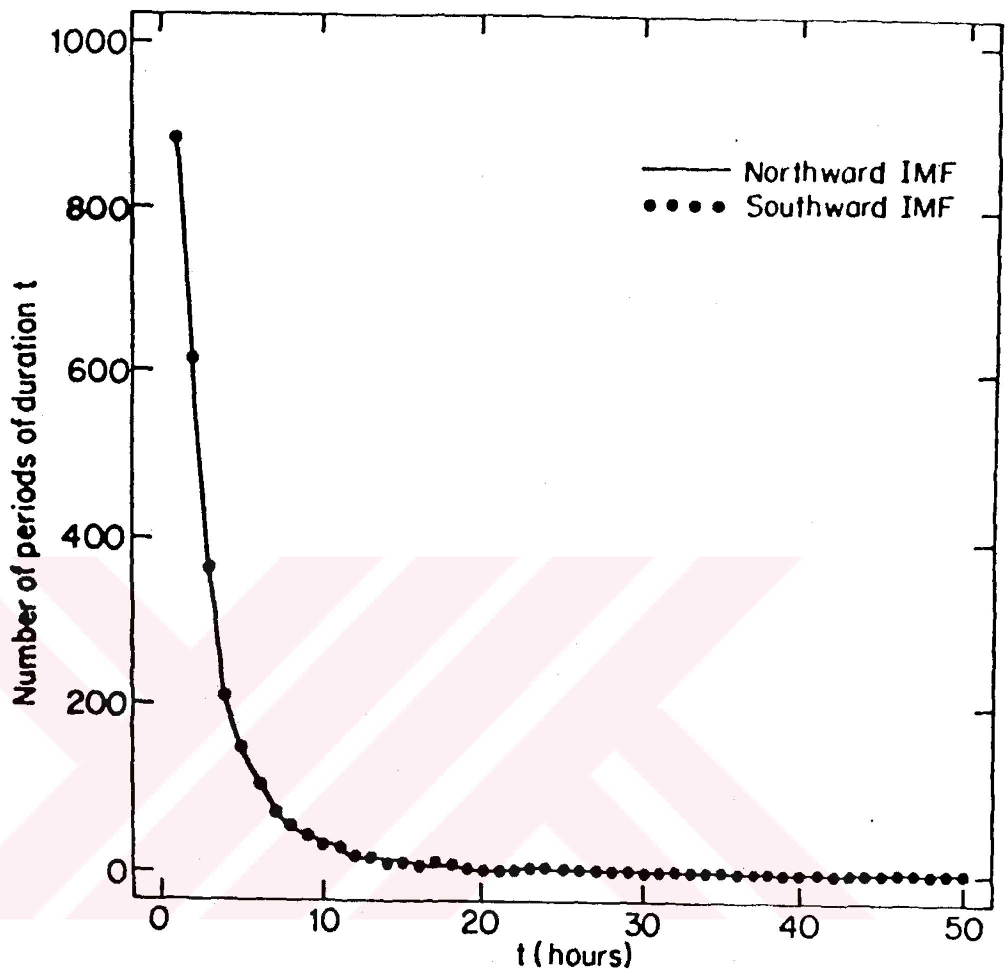

Figure 3.3 : The numbers of the IMF B_Z changes for which B_Z subsequently had a constant sense for a time t, as a function of t.

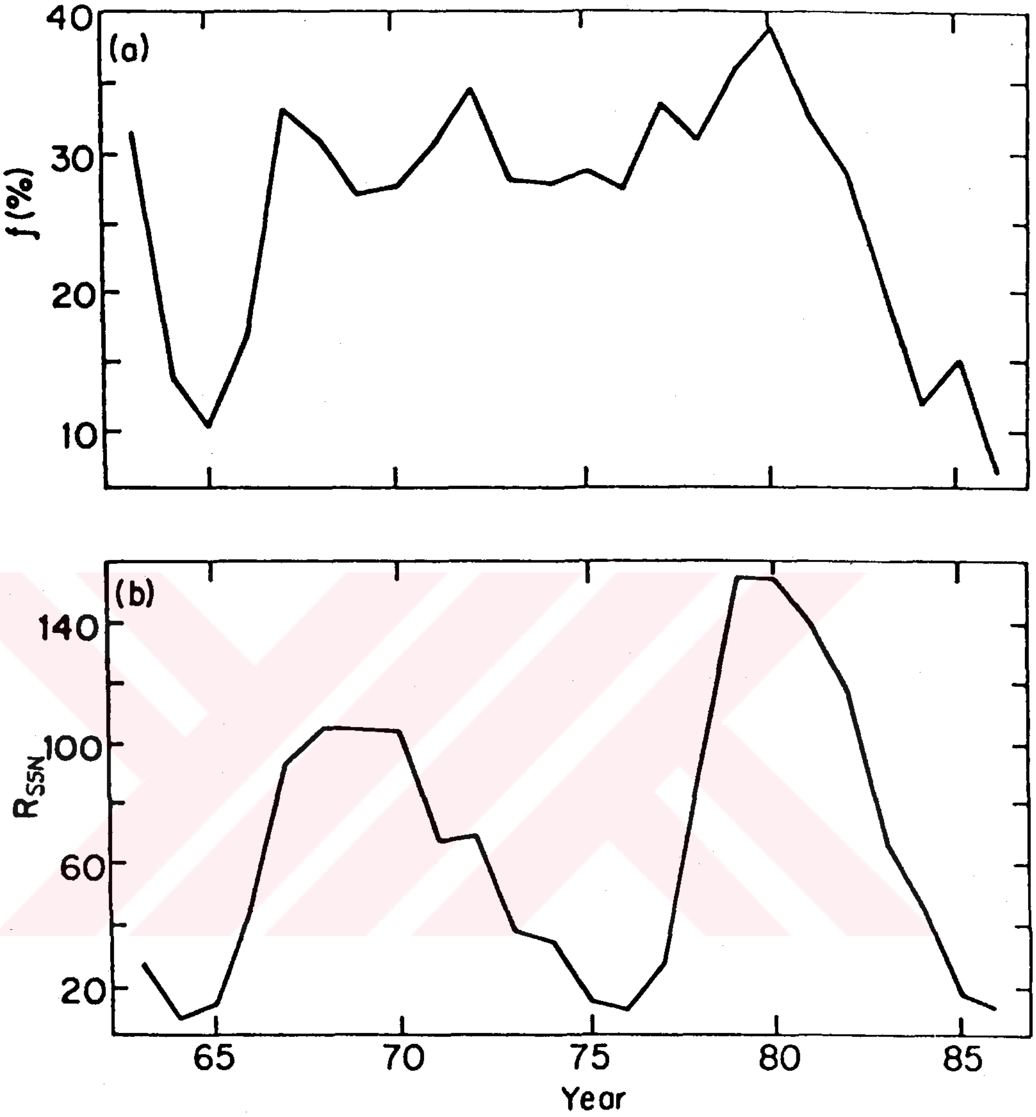

Figure 3.4 : (a) Annual fraction of cases for which B_Z had a constant sign for three or more hours following a major reversal of the B_Z sign; (b) annual sunspot numbers.

hours after a major reversal, in the case of large values of $f\%$ it might be interpreted that the solar - terrestrial system behaves in a steady state case or it shows regular oscillations around a mean value [8].

3.1.4. Dynamic Pressure Changes of Solar Wind

It was also searched whether there was any possible link between B_Z changes and changes in the dynamic pressure of the SW. Figure 3.5 is a three dimensional histogram showing the relationship between B_Z changes and fractional dynamic pressure; $\Delta P/P\%$, changes for the events detected. In this representation, ΔB_Z is the change in IMF B_Z during an "event" and $\Delta P/P$ is the percentage change in the hourly mean of the SW dynamic pressure where P is the value at t_1. Summarizing Fig. 3.5 there are two populations of events :

i - Events in which there is no significant pressure change associated with the change in the sign of B_Z. These events are represented by the prominant ridge at zero pressure change.

ii - Events in which there is a pressure change associated with the change in B_Z sign. These are represented by the broader distribution.

Note that there are no events for $B_Z < 2nT$. As shown in Fig. 3.5 the distributions are roughly symmetric about the central ridge. That is, when southward and northward turnings are accompanied by a pressure change, it was as likely to be a rise in dynamic pressure ($\Delta P > 0$), as a fall ($\Delta P < 0$). This was true for both northward and southward turnings. There was some asymmetry at large $\Delta P / P$ because P tended to be larger for falls in dynamic pressure (relating as it does to the conditions before the event). In 12% of the total events $\Delta P / P$ was zero. However, in 38% of events$|\Delta P / P|$ was less than 5% and for 58% of

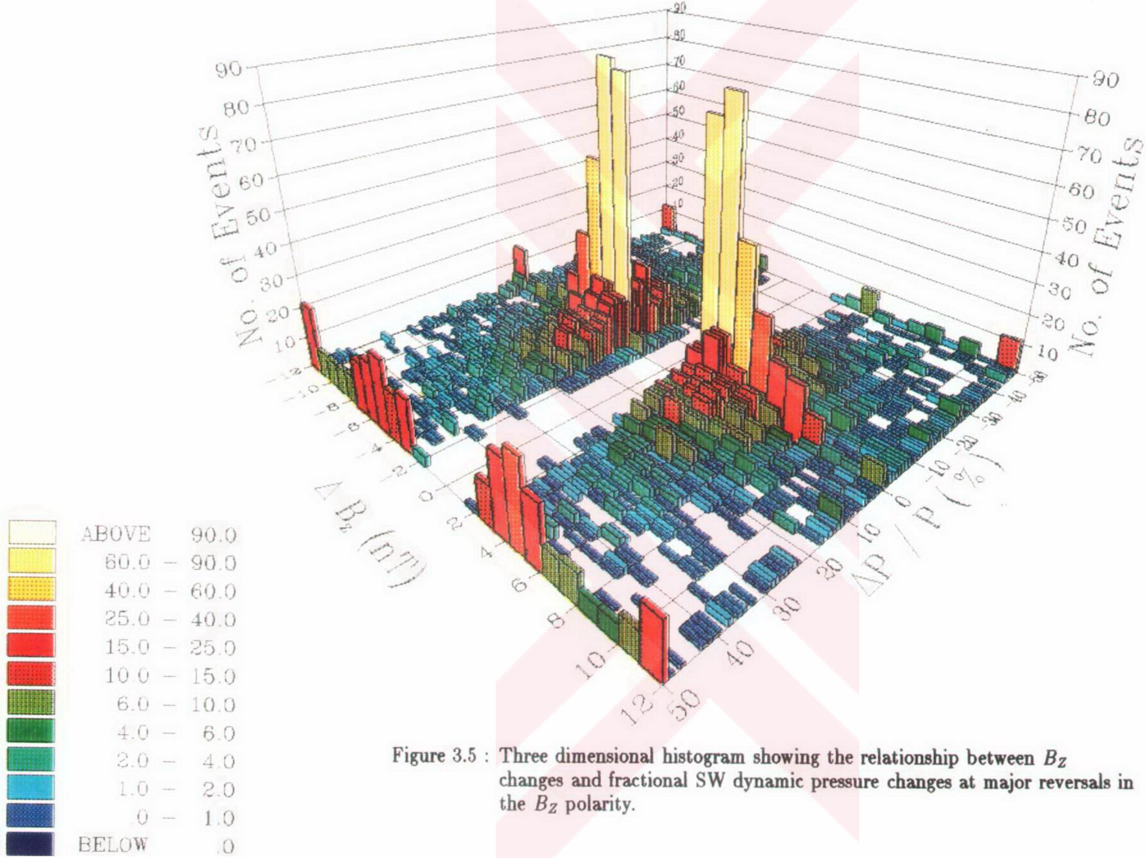

Figure 3.5 : **Three dimensional histogram showing the relationship between B_Z changes and fractional SW dynamic pressure changes at major reversals in the B_Z polarity.**

events it was less than 10%. Thus, most southward/northward turnings were not accompanied by significant (> 10 %) changes in dynamic pressure. Only 2% of total events exceeds 50% dynamic pressure changes. It is worth noting that the short term SW dynamic pressure variations ,i.e. variations taking place less than an hour, may be more responsible for the magnetospheric coupling (dayside reconnection) [8].

3.2. The Slough Ionospheric Critical Frequencies and the Interplanetary Magnetic Field Between 1967 – 1986

3.2.1 Solar Cycle Variations of the B_Z Component of IMF and the Slough $foF2$

Because of their importance to the terrestrial magnetospheric – ionospheric system [7] the solar cycle variation in the IMF B_Z and Slough $foF2$ were investigated. For each year, all hourly values of the magnitude of B_Z and $foF2$ were taken and then the mean values of $|B_Z|$ and $foF2$ were calculated. To facilitate a comparison the international sunspot numbers, R_{SSN}, were also employed. Figure 3.6 shows the variation of the (a) IMF $\overline{|B_Z|}$, (b) Slough $\overline{foF2}$, (c) Slough $\overline{\delta foF2}$ and (d) R_{SSN} in the years between 1963 and 1986. There was a clear solar cycle variation in both the mean magnitude of $|B_Z|$ and Slough $foF2$. Whereas such a variation was not very obvious in the Slough $\overline{\delta foF2}$ and R_{SSN} set. The amplitudes of the $\overline{|B_Z|}$ and $\overline{foF2}$ variations was larger in Cycle 21 than those in Cycle 20 . In each panel of Fig. 3.6 cross correlation coefficients of R as computed between $\overline{|B_Z|}$ and R_{SSN}; $\overline{foF2}$ and R_{SSN}; $\overline{\delta foF2}$ and R_{SSN} were also shown. At the significance level of $\alpha = 0.05$ if the computed R is greater than or equal to 0.38 the relationship may be interpreted as relevant. However, such a conclusion is being made with caution until such statistical conclusions are manifested with physical mechanisms or principles lying behind the data.

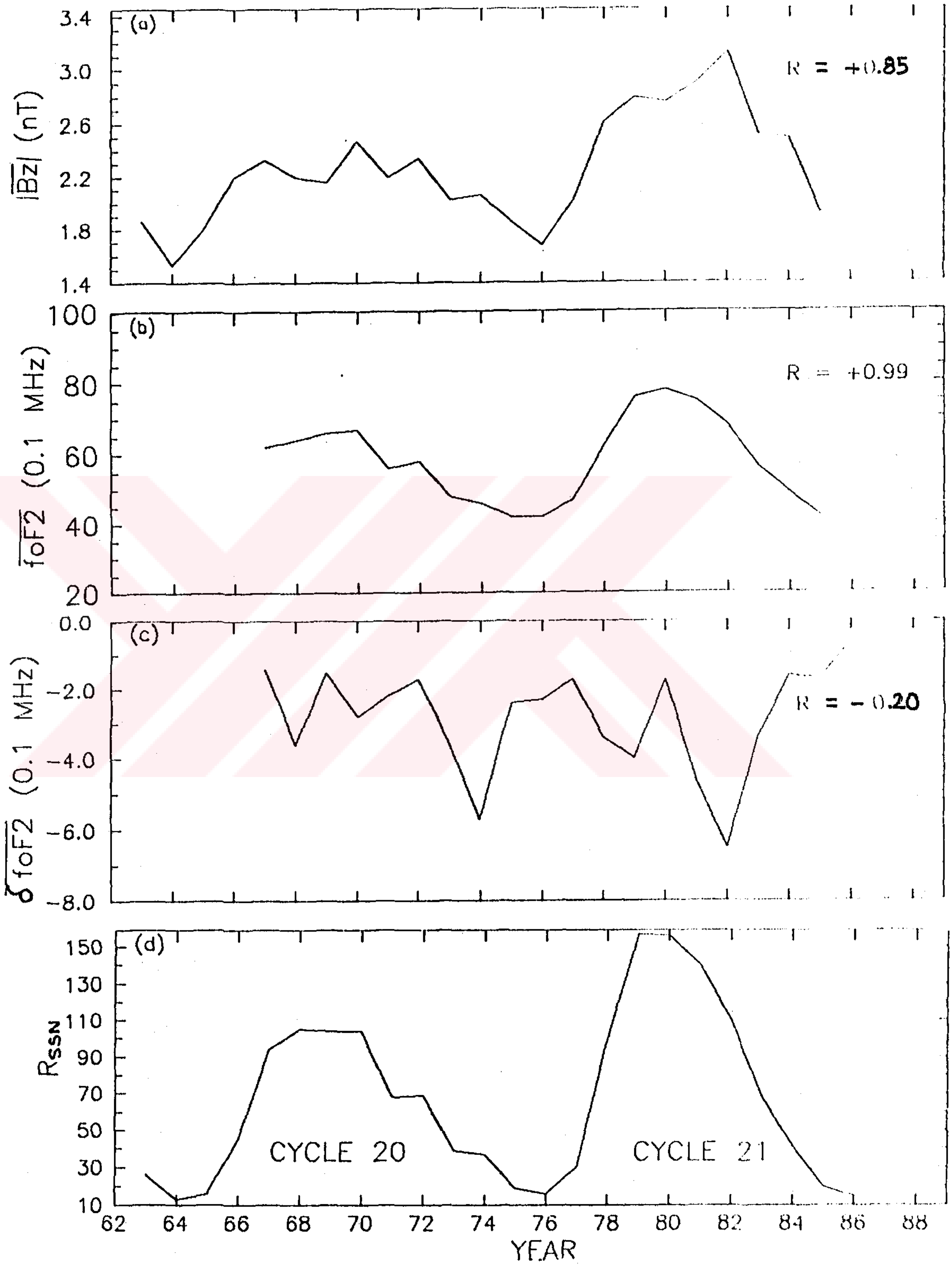

Figure 3.6 : Annual means of (a) the mean magnitude of B_Z; (b) the mean magnitude of the Slough $foF2$; (c) the mean magnitude of the Slough $\delta foF2$; (d) the annual sun spot numbers, R_{SSN}. The cross correlation coefficients between the respective data and R_{SSN} were also shown in each panel.

3.2.2. The Possible Influence of the IMF Structure On the Slough Ionospheric Critical Frequencies Between 1967 - 1986

As the electron density of the ionospheric F region is markedly controlled by the highly variable solar EUV radiation it is often impossible to seperate these phenomena from effects caused by the IMF sector structure. On the other hand the derived dates of sector boundary crossings may sometimes be erroneous [4]. Therefore, in this part of the work B_Z changes were adopted in accordance with the "event" definition. The sector structures were defined in accordance with the changes reported in the B_X component of the IMF in the data. When there was a change in the sign of the B_X component of the IMF either at the event time of t_1 or at the event time of t_2 this case was assumed as a solar sector boundary (SSB) crossing.

However, because of the uncertainities in the derivation of individual dates of sector boundary crossings only a statistical investigation carried out here. Instead of using the hourly values of the critical frequency of the $F2$ layer, $foF2$ obtained from the ionosonde station of Slough, the new set with diurnal variations removed (Section 2.2) were employed for the analysis. From here on the analysis was conducted by employing this set, i.e. $\delta foF2$.

In the following paragraphs the results of the data analysis based on the annual, diurnal variations of the Slough $\delta foF2$, and the various IMF configurations on the $\delta foF2$ will be summarized. In particular, the plots representing the effects of the IMF configuration were smoothed by the best fit 10th degree orthogonal polynomials. Fitting polynomials to the data provided a better visualisation, and an easier way of discussing the trends in the data.

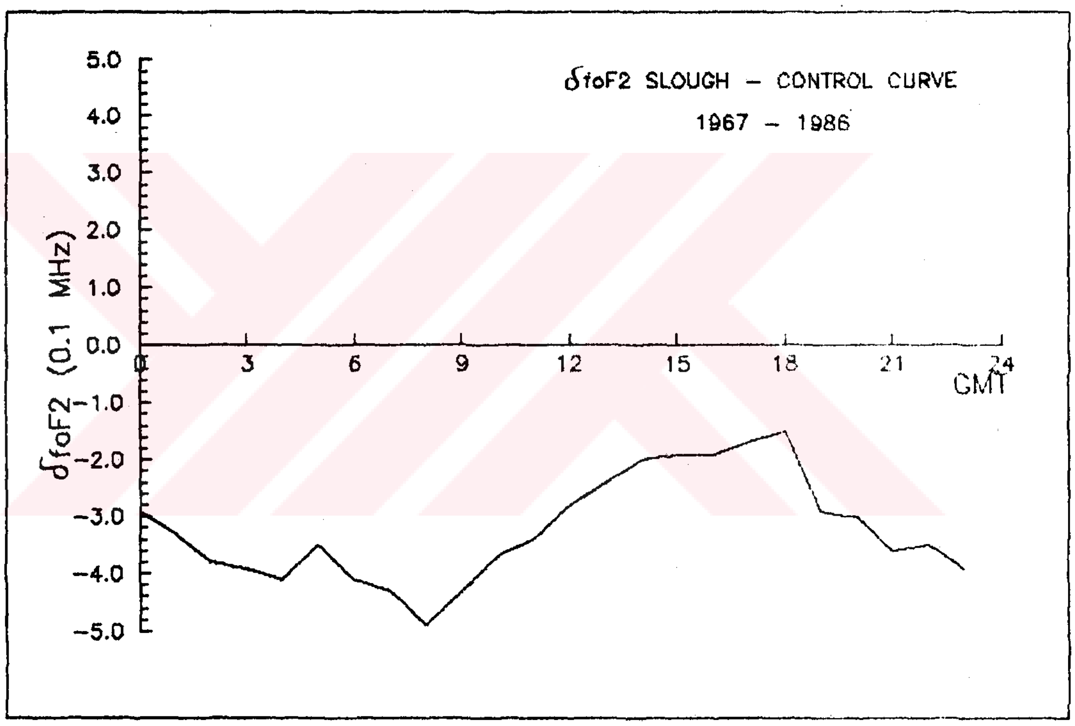

Figure 3.7 : The diurnal variation of the Slough $\delta foF2$ in the years between 1967 and 1986.

(i) Figure 3.8 exhibits the diurnal variation of the averaged Slough $\delta foF2$ data during events in the years between 1967 and 1986. There were no events recorded met the criteria defined in Section 2.4 in the years 1985 and 1986. This might have arisen due to the poor data coverage and since these years marked a low solar cycle period. These curves were constructed by taking into consideration only an eight hour long record of the Slough $\delta foF2$ centered on the event times t_1 and t_2 for each year. Then, an arithmetic average of the $\delta foF2$ for each hour was computed (referred from now on $\overline{\delta foF2}$ unless stated otherwise). From Fig. 3.8 one may feel the influence of the solar cycle variation over the years. However, due to the poor coverage it is not very easy to pin down the exact form of such a possible dependence. Therefore, Fig. 3.9a was constructed by taking the mean of the percent $\overline{\delta foF2}$s over the years between 1967 and 1986 covering the whole of the solar cycles 20 and 21. The tendency for more negative percent $\overline{\delta foF2}$ values towards cycle 21 is more obvious. However, at a significance level of $\alpha = 0.05$ a cross correlation coefficient of $R = 0.03$ between the $\overline{\delta foF2}$ and the annual sun spot numbers (R_{SSN}) imply that there is not an obvious relationship between the two independent data set. This result supports the finding expressed in Sec. 3.2.1 where $\delta foF2$ for the whole set without considering the events was compared with the variation of the sunspot numbers over the same period.

The percent diurnal variation of the Slough $\overline{\delta foF2}$ for twenty years is illustrated in Fig. 3.9b. This curve shows that the variability of the $\overline{\delta foF2}$% increases during dusk and night hours. One may also note that the $\overline{\delta foF2}$% exhibits an oscillatory behaviour.

(ii) To see the effects of the IMF B_Z turnings on the Slough $\delta foF2$, the $\delta foF2$ data were sorted out into two groups; namely, the $\delta foF2$ during the events with a southward IMF turning, and the $\delta foF2$ during the events with a northward

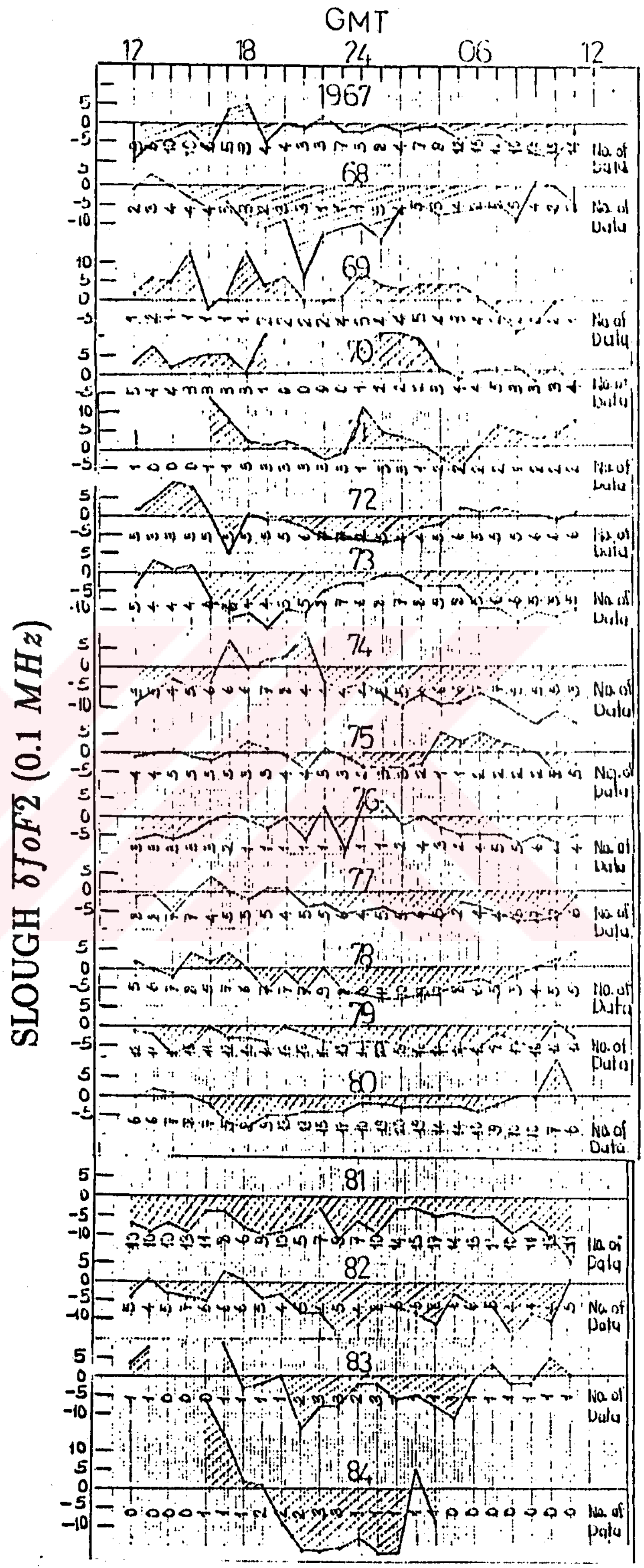

Figure 3.8 : The diurnal variation of the Slough $\overline{\delta foF2}$ during events in the years between 1967 and 1986.

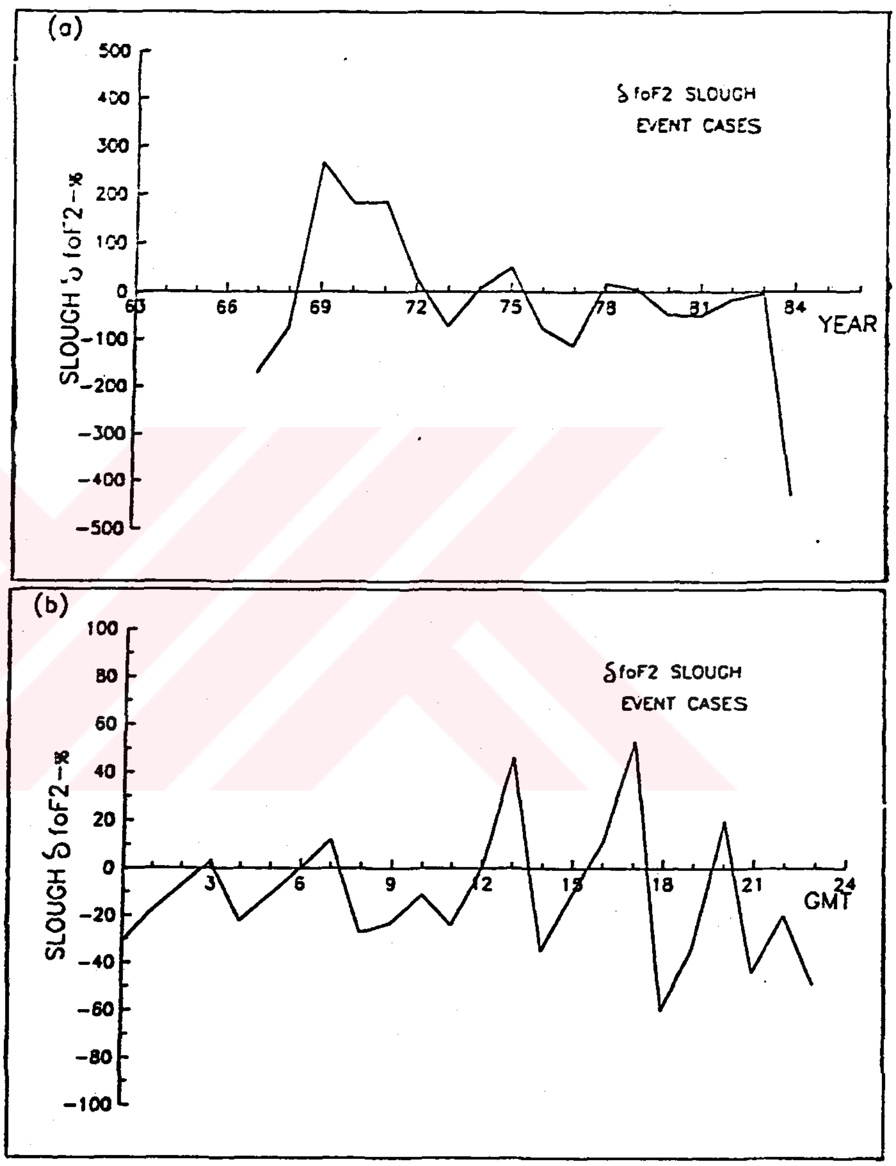

Figure 3.9 : (a) The percent annual variation (b) the percent diurnal variation of the Slough $\overline{\delta foF2}$ during events in the years between 1967 and 1986. The percent was computed by employing the control curve of Fig. 3.7.

IMF B_Z turning. Figure 3.10a,b shows the diurnal percent variation of the mean $\delta foF2$ between 1967 and 1986 for two seperate IMF B_Z turnings (southward and northward) during the events. In this representation of the $\delta foF2$ variations the solar sector transitions were not taken into consideration. The data for each hour were gathered by recording the $\delta foF2$ values measured within an eight hour interval of the event time t_2. Then an arithmetic average of the $\delta foF2$ values were computed as explained above in the previous paragraphs for each hour. The data, then, were normalized by taking into consideration the control curve of the $\overline{\delta foF2}$ of Fig. 3.7. The best fit curves were superimposed in panel (c) of Fig. 3.10. At the significance level of $\alpha = 0.05$ both sets of $\overline{\delta foF2}\%$ values were not correlated. Magnitudewise, during the events when the IMF oriented from north to south $\overline{\delta foF2}\%$ values seem to become greater almost at all hours compared to those cases associated with the south to north IMF turnings. Both sets of $\overline{\delta foF2}\%$ curves exhibit an expected diurnal variation with a tendency to increase during day times. In addition, the southward IMF induced $\overline{\delta foF2}$ values which were greater than the corresponding control curve values. On the other hand, northward turnings of the IMF induced $\overline{\delta foF2}$ values which were smaller than the control curve values. It may, thus, be concluded that the north/south differences in the IMF markedly have got some control on the ionospheric critical frequencies.

(iii) In order to understand the effect of the direction of the IMF B_X component (i.e. IMF sector structure) on the Slough $\delta foF2$, the data were sorted out into four groups: the $\delta foF2$ during the events of a southward IMF B_Z turning with T and A polarities; $\delta foF2$ during the events of a northward IMF B_Z turning with T and A polarities. Then, as explained above, the percent changes with respect to the control curve (Fig. 3.7) were then calculated for each group.

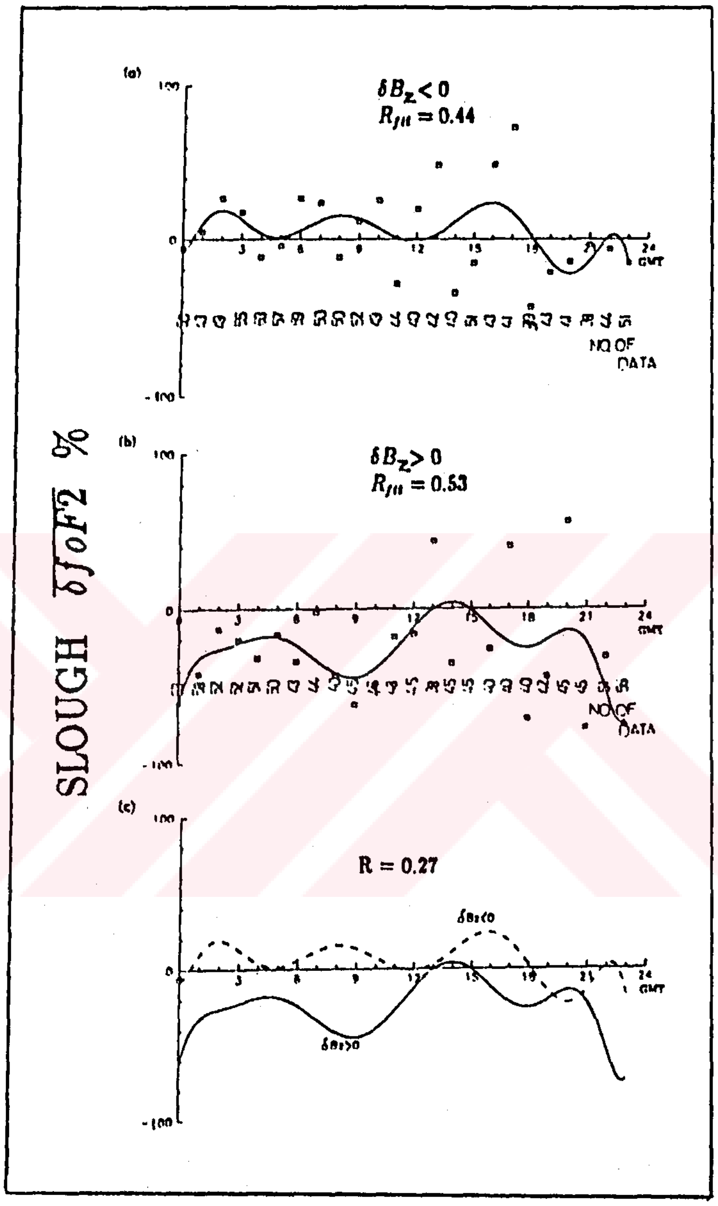

Figure 3.10 : The effects of the IMF B_Z turnings on the Slough $\overline{\delta foF2}\%$.

Figure 3.11a,b,d,e show the diurnal percent variation of the mean $\delta foF2$ between 1967 and 1986 for the two seperate IMF B_Z turnings with two seperate IMF B_X polarities. Figure 3.11a,b show the IMF B_X polarity differences in the diurnal $\overline{\delta foF2}$% variation for the southward IMF. The best fitted curves were superimposed in Fig. 3.11c in order to illustrate the effect of the direction of the IMF B_X polarity. It was found out that two sets of data were anticorrelated at a significance level of $\alpha = 0.05$. It was also found out that an IMF with A polarity induced $\overline{\delta foF2}$ values which were greater than the control curve values whereas an IMF with T polarity induced $\overline{\delta foF2}$ values which were smaller than the control curve values for the southward IMF B_Z turnings.

Figure 3.11d,e show the IMF B_X polarity differences in diurnal $\overline{\delta foF2}$ variation for events with a northward IMF B_Z turning. In Fig. 3.11f these two figures were superimposed in order to see the effect of the IMF B_X polarity. From this representation it was found out that when IMF directed northward the curves representing the changes of the $\overline{\delta foF2}$ for T and A polarities were negatively correlated at a significance level of $\alpha = 0.05$. For A polarity, on the other hand, $\overline{\delta foF2}$ values were greater than the control curve values in day times (08-20)GMT and smaller in other hours whereas for T polarity cases $\overline{\delta foF2}$ values were almost smaller than the control values at all hours.

Figure 3.11g,h show the percent variation of the $\overline{\delta foF2}$ for two seperate IMF B_Z turnings for A and T sectors. For T polarity the $\overline{\delta foF2}$ values were smaller than the control values for both IMF B_Z turnings almost at all hours. Magnitudewise, in day light times the events with a southward IMF B_Z turning induced greater $\overline{\delta foF2}$ values than the events with a northward IMF B_Z turning did for T polarity.

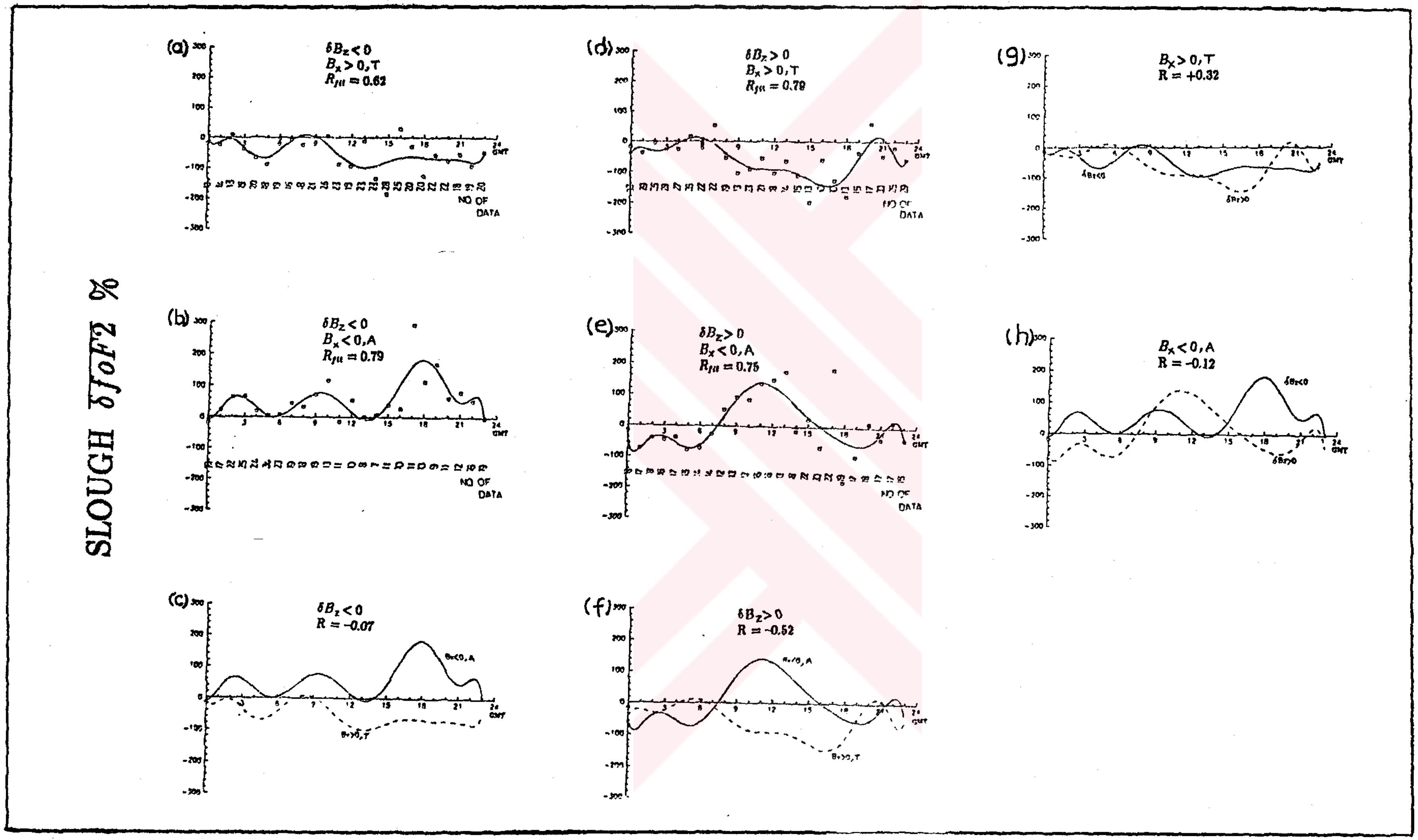

Figure 3.11 : The effects of the direction of the IMF B_X component (IMF sector structure) on the Slough $\overline{\delta foF2}$%.

In order to develop some means of comparison, the cross correlation coefficients computed between the distinct groups were listed in Table 3.2.

Table 3.2.

The cross correlation coefficients between the distinct groups.

$R_{A\ polarity...T\ polarity}$		$R_{\downarrow B_z...\uparrow B_z}$	
$\downarrow B_Z$	$\uparrow B_Z$	A Polarity	T Polarity
−0.073	−0.52	−0.12	+0.32

To summarize the result of the analysis: the direction of the IMF B_Z turnings seems to be relevant in the diurnal variation and the magnitudes of the $\overline{\delta foF2}$. i.e. the $|\overline{\delta foF2}|$ values are greater for the events with a southward IMF turning than those of the northward IMF turning . When the IMF B_Z turning is southward, the polarity of B_X also seem to be relevant. This situation was not very obvious when the IMF turns northward.

(iv) The effects of the solar sector boundary (SSB) crossings – the reversal of the polarity of the IMF B_X component between the event time of t_1 or t_2 – on the Slough $\delta foF2$ were searched by sorting out the $\delta foF2$ data into four groups namely the $\delta foF2$ values obtained during the events of the southward IMF turning with (T to A) transitions, and (A to T) transitions; the $\delta foF2$ values obtained during the events of northward IMF turning with (T to A) transitions, and (A to T) transitions. Again, the percent variations of the $\overline{\delta foF2}$ with respect to the control curve of Fig. 3.7 (for each group) were, then, calculated. Due to the restrictions improved on the selection of an event, during sector transitions there have been a small number of event cases detected in the 20 year long data. Therefore, the statistics is very poor. Figure 3.12a,b,d,e show the diurnal percent variation of the mean $\overline{\delta foF2}$ between 1967 and 1986 for two seperate IMF B_Z turnings with two types of SSB crossings.

Figure 3.12a,b show the SSB crossing effects on the $\overline{\delta foF2}\%$ in the case of the southward IMF turnings. In Fig. 3.12c these two curves were superimposed in order to investigate the effects of the different SSB crossings on the $\overline{\delta foF2}\%$ variation. It can be seen that two curves are positively correlated at a significance level of $\alpha = 0.05$. This may imply that (A to T) and (T to A) SSB crossings (or transitions) seem to produce similar effects on the $\delta foF2$ in the case of southward IMF turning. During both types of the SSB crossings there were enhancements of the Slough critical frequencies with respect to the midday hours. On the other hand, it may be seen from Fig. 3.12c that (A to T) SSB crossings induced greater $\overline{\delta foF2}$ values than (T to A) SSB crossings did almost at all hours.

Figure 3.12d,e show the SSB crossing effects on the Slough $\overline{\delta foF2}\%$ during the events with northward IMF turnings. In Fig. 3.12f the two best fit curves were superimposed in order to investigate the probable effects of the different SSB crossings on the $\overline{\delta foF2}$. As the cross correlation coefficients computed indicate at a significance level of $\alpha = 0.05$, the $\overline{\delta foF2}$ values for these two sets did seem to be anticorrolated. On the other hand, the $\overline{\delta foF2}$ variations during the (A to T) SSB crossings lagged behind the $\overline{\delta foF2}$ variations during the (T to A) SSB crossings by about 6 hours. Magnitudewise, $\overline{\delta foF2}$ values during the (A to T) SSB crossings were greater than those of the (T to A) SSB crossings in general.

Figure 3.12g,h show the percent variation of the $\overline{\delta foF2}$ for two IMF B_Z turnings during the two seperate SSB crossings. For the (T to A) SSB crossings, opposite B_Z turnings seemed to produce antisymmetrical enhancements in the $\overline{\delta foF2}\%$ values between (5-21)GMT implying that IMF B_Z turnings do matter. Whereas for the (A to T) SSB crossings one may observe somehow a more similar variations in the Slough $\delta foF2$ data. Magnitudewise, on the other hand, an IMF with southward turning produced greater $\overline{\delta foF2}$ values than an IMF with northward IMF turning

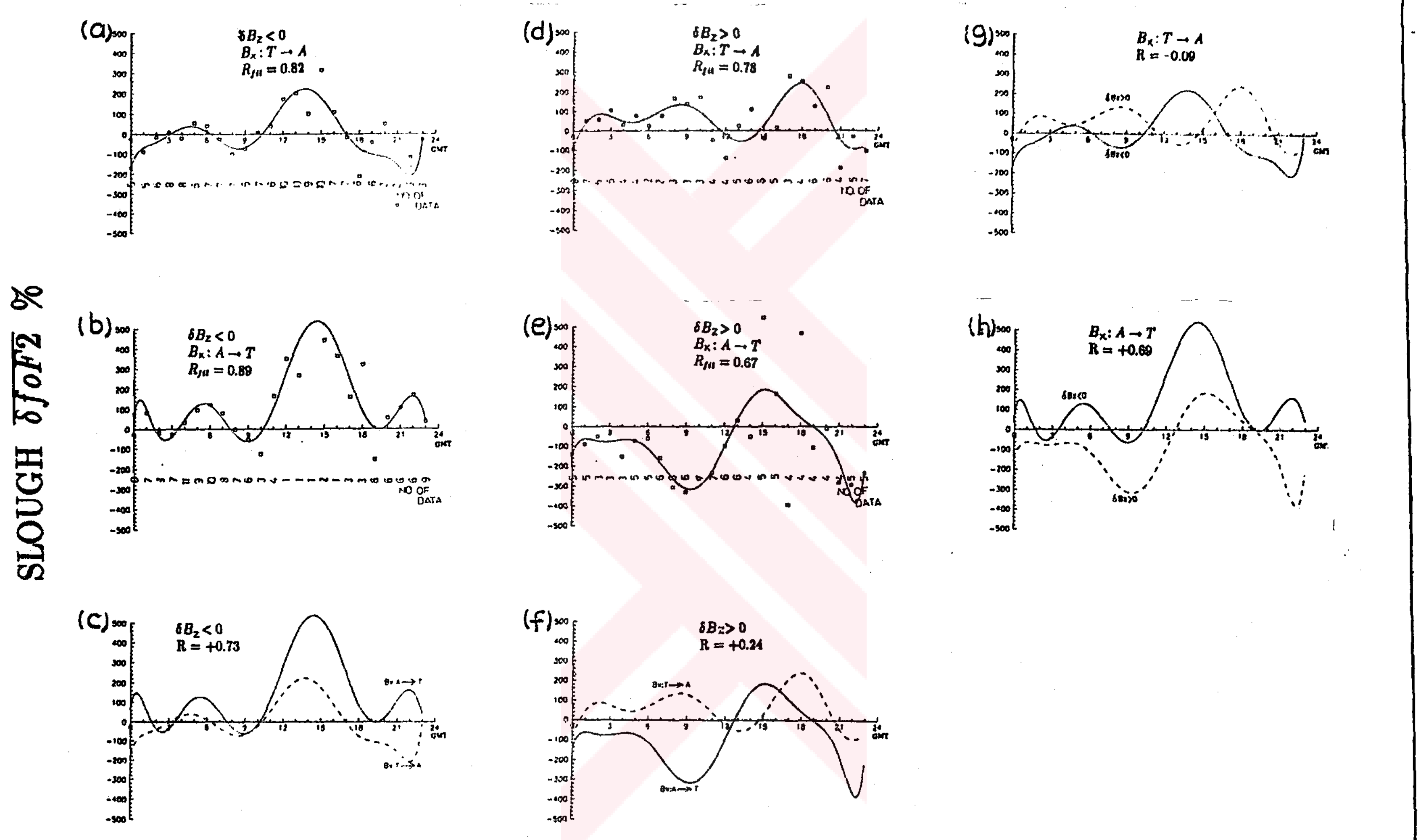

Figure 3.12 : The effects of the solar sector boundary (SSB) crossings on the Slough $\overline{\delta foF2}$%.

did in the case of (A to T) SSB crossings.

The cross correlation coefficients between the distinct groups were listed in Table 3.3.

Table 3.3.

The cross correlation coefficients between the distinct groups.

$R_{A\rightarrow T...T\rightarrow A}$		$R_{\downarrow B_z...\uparrow B_z}$	
$\downarrow B_Z$	$\uparrow B_Z$	A → T	T → A
+0.73	+0.24	−0.09	+0.69

Summarizing once more, during the unsteady variations of the IMF B_X component the southward IMF B_Z component seem to dominate the Slough $\overline{\delta foF2\%}$ values more than those of the B_X polarity reversals. In the case of a northward IMF B_Z turning B_X reversals seem to be more dominant over the Slough $\overline{\delta foF2\%}$ values.

During the (T to A) B_X reversals again B_Z control is more dominant. Whereas during the (A to T) B_X reversals the direction of the SSB crossing seem to be more relevant.

CHAPTER 4

GENERAL CONCLUSIONS AND FURTHER SUGGESTIONS

The following results obtained throughout this work:

Southward and northward turnings of the IMF were found in almost equal frequencies (51% and 49% respectively). 24 % of the events, the IMF B_X and B_Y did not change their signs between $(t_1 - 3\text{h})$ and $(t_2 + 3\text{h})$ (t_1 and t_2 are event times). Only for 9% of the events there were either B_X or B_Y reversal during an event. During a B_Z reversal, most of the time the horizontal IMF component, B_{XY} in the ecliptic plane was either in the second or in the fourth quadrant of the (X,Y) cartesian coordinate system.

The vertical component, B_Z, of the IMF in the GSM coordinate system showed some systematic variations due to the diurnal and seasonal changes of the earth's dipole axis with respect to the solar rotation axis. It was shown that an IMF with A polarity ($B_X < 0$) induced positive B_Z values during the spring half year (January to June) and negative B_Z values during the autumn half year (July to December); whereas, an IMF with T polarity ($B_X > 0$) caused a symmetrical picture in B_Z variation. Meanwhile, the diurnal B_Z variation had smaller amplitudes than those of the seasonal B_Z component. There was found a time lag of about 12 hours between A and T polarities for both types of B_Z cases ($B_Z < 0$ –Pro sectors–; and $B_Z > 0$ –Anti sectors–). From this analysis, it can be seen that in deciding the diurnal B_Z variation both in the Anti and Pro sectors, the polarity of the sector structure was the dominant factor. The results obtained here were mostly consistent with those of the published ones. In particular, the results reported here were extended the theoretical findings which had been based on a spherically expanding steady – state solar wind adopted by Bremer (1988) [4]. A similar analysis could be carried out by employing the IMF B_Y component. It is important, again, to note that the IMF were mostly either in the 2nd or in the 4th quadrants of the GSM cartesian coordinate system. Therefore, it is expected to find somehow a symmetrical behaviour of the IMf if only the B_Y component were used.

In 12.2 % of the cases detected, following an event, the B_Z component was stable for a period of more than 2 hours. Meanwhile, a solar cycle effect was observed on this stability. Since the southward IMF turning plays a major role in the coupling of the the solar wind and magnetosphere [9], it is important to determine the stable IMF B_Z condition. After a B_Z reversal, if B_Z keeps its sign for a definite length of time (here, it was assumed more than 2 hours), the solar – terrestrial system behaves in a steady state case or it shows regular oscillations around a mean value. On the other hand, if the IMF B_Z component varies on time scales shorter than (or comparable with) the response time of the terrestrial system, there will not be a steady case or a regular oscillation. Since the percentage of the number of stable IMF B_Z cases are small (12. 2 % of total number of hours) the ionosphere–magnetosphere system is very rarely at a steady – state case.

There were not found significant high solarwind dynamic pressure changes during the IMF B_Z reversals (only 2 % of the total events exceeded 50% dynamic pressure changes). When the SW encounters the geomagnetic field, it exerts a dynamic pressure on it. Since the cases in which IMF B_Z reversals occured are the candidates for the magnetospheric coupling (reconnection) [6,9], the dynamic pressure must change markedly during these reversals. Since the hourly values of the IMF and the SW parameters were used in this work, it was not possible to see any probable effects on the IMF – magnetosphere – ionosphere coupling clearly. In other words, as reported elsewhere [8], shorter SW dynamic pressure changes are more likely responsinle for the magnetospheric coupling [8].

As expected, the clear solar cycle variation observed in the Slough $foF2$ data were not explicitely seen in the $\delta foF2$ data. However, amplitudewise there was a very prominent difference in both $foF2$ and $\delta foF2$ data when the solar cycle 20 was compared with the solar cycle 21. The amplitude of the $foF2$ data was larger in cycle 21 than those of the cycle 20.

The possible effects of the IMF configuration on the ionospheric critical frequency, $foF2$, investigated by employing the eight–hour long record of the Slough $\delta fof2$ data centered on the events. It was shown that north/south differences in the IMF have got some control over the ionospheric critical frequencies. That is, when the IMF oriented north to south $\overline{\delta foF2}\%$ values seemed to become more greater almost at all hours compared to those cases associated with the south to north IMF turnings. In addition, the southward turnings of the IMF induced greater $\overline{\delta foF2}$ values were greater than the corresponding control curve values.

It was found out that in the case of southward IMF turnings, the IMF sector structure also seemed to have some control over the distribution of the Slough $\overline{\delta foF2}\%$. This situation was not very obvious in the case of northward IMF turnings. Meanwhile, for the southward IMF turning, an IMF with A polarity induced $\overline{\delta foF2}$ values which were greater than the corresponding control curve values; whereas an IMF with T polarity induced $\overline{\delta foF2}$ values which were smaller than the corresponding control curve values.

During the unsteady variations of the IMF B_X component (sector transitions) the southward IMF B_Z component seemed dominate the Slough $\overline{\delta foF2}$ values more than those of the B_X polarity reversals. On the other hand, in the case of a northward B_Z turning B_X reversals seemed to be more dominant over the Slough $\delta foF2$. During the (T to A) B_X reversals, again, B_Z control was more dominant. Whereas, during the (A to T) B_X reversals the direction of the SSB crossing seemed to be more relevant.

REFERENCES

[1] JURSA, A.S. (ed.), Handbook of Geophysical and the Space Environment, USAF (1985)

[2] ROY, A.E. and D. CLARKE, Astronomy, Adam Hilger Ltd., Bristol (1982)

[3] ZIRIN, H., The Solar Atmosphere, Blaisdell Publishing Company, Massachusetts (1966)

[4] BREMER, J., The influence of the IMF structure on the ionospheric F region, Journal of Atmospheric and Terrestrial Physics, 50, 831-838 (1988)

[5] HERMAN, J.R. and R.A. GOLDBERG, Sun, Weather and Climate, NASA, Washington (1978)

[6] HESS, W.N., The Radiation Belt and Magnetosphere, Blaisdell Publishing Company, USA, Massachusetts (1968)

[7] RATCLIFFE, J.A., Sun, Earth and Radio, World University Library, London (1970)

[8] HAPGOOD, M.A., Y.K. TULUNAY, M. LOCKWOOD, G.A. BOWE and D.M. WILLIS, Variability of the interplanetary medium at 1 AU over 24 years : 1963-1986, Planetary Space Sciences [Accepted for publication] (1990)

[9] NISHIDA, A., IMF control of the earth's magnetosphere, Space Science Reviews, 34 , 185-200 (1983)

[10] RISHBETH, H. and O.K. GARRIOT, Introduction to Ionospheric Physics, Acedemic Press, London (1969)

[11] GLASSTONE, S., Sourcebook on the Space Sciences, D. Van Nostrand Company, Inc., Princeton, USA (1965)

[12] BRADLEY, P.A., Improvements in mapping the critical frequency of the F2 layer, COSPAR XXVII Planetary Meeting, Helsinki (1988)

[13] RISHBETH, H., Basic physics of the ionosphere : a tutorial review Journal of the Institution of Electronic and Radio Engineers, 58, S207-S223 (1988)

[14] TULUNAY, Y.K., The topside ionosphere as observed by the satellite Ariel 3, Ph.D., Birmingham University, Space Research Department, UK (1972)

[15] RATCLIFFE, J.A., An Introduction to the ionosphere and magnetosphere, Cambridge University Press, London (1972)

[16] ARAVINDAN, P. and K.N. IYER, Day-to-day variability in ionospheric electron content at low latitudes, Planetary Space Sciences, 38, 743-750 (1990)

[17] MENDILLO, M. and K. SCHATTEN, Influence of Solar Sector Boundaries on Ionospheric Variability, Journal of Geophysical Research, 88, 9145-9153 (1983)

[18] ZEVAKINA, R.A. and E.V.LAVROVA, On the Possibility to Predict variations in the F2 - Region Parameters as a function of the IMF direction, in Solar-Terrestrial Predictions Proceedings, 4, C27-C36, National Oceanic and Atmospheric Administration, Boulder, Colo., (1980)

[19] KING, H.J., Interplanetary Medium Data Book, NSSDC/WDC, Maryland (1977)

[20] HAPGOOD, M.A., World Data Centre Databases, RAL Astrophysics and Geophysics Division, London, UK (1988)

APPENDIX A

DEFINITION OF $\delta foF2$ USED IN THE ANALYSIS

The following procedure was followed to obtain $\delta foF2$:

1. The times of "events" (turnings of IMF B_z) are those identified by the NAT3–MAG FORTRAN program and stored in EVNT DATA.
2. For each event it was first constructed a control data set by averaging $foF2$ values over geomagnetically quiet days close to event :
    - The mean daily value of the geomagnetic activity index Ap for each day from 15 days before the event to 15 days after the event were taken.
    - Out of these 31 days, days which have $Ap < 6$ was selected as "quiet days".
    - The mean $foF2$ value, then, was found for each hour of day, over the selected days. This was the "control curve" for the daily variations of $foF2$.
    - Within the quiet days, there would be occasions when no numeric value of $foF2$ was recorded. These cases were excluded from the calculation of the mean.
    - If there were no days with $Ap < 6$, there was no control curve and so, the event was eleminated from the analysis.
3. Next, the $foF2$ values to be converted to $\delta foF2$ values were selected.
4. Then, $\delta foF2$ values were calculated by substracting from each of the $foF2$ values, the value of control curve at the time of day was recorded.
5. Within these values, there would be occasions when no numeric value of $foF2$ was recorded. In these cases, $foF2$ values were treated as absent data values set an absent data value 999.

By substracting the control curve, it was attempted to remove diurnal variations from the data set. Thus it was assumed that the $\delta foF2$ array was free of diurnal effects.

APPENDIX B

COMPUTER PROGRAM TO DETECT THE EVENTS

```
!!!!!!!!!!!!!!!!!!!!!!!!!!!!!!!!!!!!!!!!!!!!!!!!!!!!!!!!!!!!!!!!!!!!!!!!
! This program was last checked on Wednesday, Oct. 3rd of 1989         !
! It was also compiled with the VSFORTRAN Compiler,version 2.          !
! It needs at least 3.2 MByte virtual storage to be run.               !
! Constructed by Orhan Gokcol       Istanbul Teknik Universitesi (ITU) !
!                                                                      !
!                  R E V I S E D    P R O G R A M                      !
!                                                                      !
!                  It also prepares NEWGAP DATA file                   !
!                                                                      !
!!!!!!!!!!!!!!!!!!!!!!!!!!!!!!!!!!!!!!!!!!!!!!!!!!!!!!!!!!!!!!!!!!!!!!!!
!!!!!!!!!!!!!!!!!!!!!!!!!!!                 !!!!!!!!!!!!!!!!!!!!!!!!!!!!
!!!!!!!!!!!!!!!!!!!!!!!!!!!                 !!!!!!!!!!!!!!!!!!!!!!!!!!!!
!!!!!!!!!!!!!!!!!!!!!!!!!!!!!!!!!!!!!!!!!!!!!!!!!!!!!!!!!!!!!!!!!!!!!!!!
      Real Bx(5),By(5),Bz(5),Sx(5),Sy(5),Sz(5),Ssx(8500),Bbx(8500)
      Real Ssy(8500),Ssz(8500),Bby(8500),Bbz(8500)
      Integer Ysi(20,900),Xsi(20,900),Six(20,900),Siy(20,900)
      Integer Month(5),Day(5),Hour(5),Num(5),Gap(20,0:50),Llin(900)
      Integer Hhour(8500),Dday(8500),Mmon(8500),Szbil(20,900)
      Integer Egim(20,900),Line(20,900),Yil(20),T,Gi,Dt,Slp
      Integer Ay(20,900),Gun(20,900),Saat(20,900),Year,Count,W
      Integer GapA(20,0:1,50),Gap3(0:1,50),Gap2(0:50)
      Integer Evgap(900),Evngap(20,900),Jbz(-15:15)
      Integer Ibz1(-15:15),Ibz2(-15:15)
      Integer Mag_un,Evn_un,Gap_Un,Gapi_Un
      Logical Lg,Lg1,Lg2,Lg3
      Parameter (Bz_val=1.0,W=0)
!
! Screen logo----
      Print*,'Explanations for st. deviation parameter of Bz  (Isz):'
      Print*,'Cases in which the absolute value of Bz is greater than 2*
     &Sz, type 2 for Isz'
      Print*,'Cases in which the absolute value of Bz is greater than 1*
     &Sz, type 1 for Isz'
      Print*,'Otherwise, type 0 for Isz'
      Print*,'Now,type Isz value........(0 or 1 or 2)'
!
      Read*,Isz
!!!!!!!!!!!!!!!!!!!!!!!!!!!!!!!!
      Data Iend/20/
!!!!!!!!!!!!!!!!!!!!!!!!!!!!!!!!
      Data T,Dt,Evn_un,Gap_Un,Gapi_Un/1,2,71,77,78/
      Dt1=Float(Dt)
      Do 333 Iy=1,Iend
      Print*,1985-Iy
      Mag_un=Iy+10
      Iv=Dt
      Nn=0
      Count=0
!
! Read the IMF parameters from MAG** DATA
120   Do 100 I=T,Dt
      Read (Mag_un,107,End=200) Year,Month(I),Day(I),Hour(I),
     &                          Bx(I),By(I),Bz(I),Sx(I),Sy(I),Sz(I)
      Count=Count+1
        If (Isz*Sz(I).lt.Abs(Bz(I))) Then
            Ibz=Nint(Bz(I))
            If (Ibz.gt.15) Ibz=15
            If (Ibz.lt.-15) Ibz=-15
            Jbz(Ibz)=Jbz(Ibz)+1
        End If
      Bbx(Count)=Bx(I)
      Bby(Count)=By(I)
      Bbz(Count)=Bz(I)
      Ssx(Count)=Sx(I)
      Ssy(Count)=Sy(I)
```

```
      Ssz(Count)=Sz(I)
      Mmon(Count)=Month(I)
      Dday(Count)=Day(I)
      Hhour(Count)=Hour(I)
      Num(I)=Count
100   Continue
        If (Isz.eq.0) Then
           Lg=.True.
        Else If (Isz.eq.1) Then
            Lg=(Abs(Bz(1)).gt.Sz(1)).and.(Abs(Bz(2)).gt.Sz(2))
        Else If (Isz.eq.2) Then
           Lg=(Abs(Bz(1)).gt.2*Sz(1)).and.(Abs(Bz(2)).gt.2*Sz(2))
        End If
      T=2
      If (Lg) Then
      Do 101 I=2,Dt
      Ih2=Hour(I)
*
* If two data don't belong to same day, call the 'DATE  Subroutine'
* which arranges this type of data
        If ((Day(I).ne.Day(1)).or.(Month(I).ne.Month(1))) Then
          Call Date (Month(1),Month(I),Day(1),Day(I),Year,61)
          Ih2=Ih2+24*61
        End If
      Lg1=(Ih2-Hour(1)).eq.1
      Lg2=Abs(Bz(1)).gt.Bz_val
      Lg3=Abs(Bz(I)).gt.Bz_val
*
* There is an event when the absolute values of Bz1 and Bz2 are greater
* than 1 nT and t2-t1=dt and the parameter NC=2
        If (Lg1.and.Lg2.and.Lg3) Then
          Call Start (Bz(1),Bz(I),Dt1,Slp,Nc)
           If (Nc.eq.2) Then
               Nn=Nn+1
               Ay(Iy,Nn)=Month(I)
               Gun(Iy,Nn)=Day(I)
               Saat(Iy,Nn)=Hour(I)
*
*   Positive Bz-slope :slp=1 ; Negative Bz-slope :slp=0
               Egim(Iy,Nn)=Slp
               Line(Iy,Nn)=Num(I)
               Llin(Nn)=Num(I)
      If((Isz*Sz(I).lt.Abs(Bz(I))).and.(Isz*Sz(1).lt.Abs(Bz(1)))) Then
            Ii=Nint(Bz(I))
            Ij=Nint(Bz(I-1))
            If (Ii.gt.15) Ii=15
            If (Ii.lt.-15) Ii=-15
            If (Ij.gt.15) Ii=15
            If (Ij.lt.-15) Ii=-15
            Ibz1(Ii)=Ibz1(Ii)+1
            Ibz2(Ii)=Ibz2(Ij)+1
        End If
*
* Check the st. dev. of Bz.
            Szbil(Iy,Nn)=0
            Lg1=(Sz(I).lt.Abs(Bz(I))).and.(Sz(1).lt.Abs(Bz(1)))
            Lg2=(2*Sz(I).lt.Abs(Bz(I))).and.(2*Sz(1).lt.Abs(Bz(1)))
            If (Lg2) Then
               Szbil(Iy,Nn)=2
            Else If (Lg1) Then
               Szbil(Iy,Nn)=1
            End If
          End If


        End If
101   Continue
      End If
```

```
      Do 102 I=2,Dt
      II=I-1
      Bx(II)=Bx(I)
      By(II)=By(I)
      Bz(II)=Bz(I)
      Sx(II)=Sx(I)
      Sy(II)=Sy(I)
      Sz(II)=Sz(I)
      Hour(II)=Hour(I)
      Day(II)=Day(I)
      Month(II)=Month(I)
      Num(II)=Num(I)
102   Continue
      Goto 120
200   Yil(Iy)=Year
      Call Sign(Mmon,Dday,Hhour,Year,Line,Count,Nn,Egim,1,Xsi,Szbil,Bbx,
     &Ssx,Six,Sign_Un,Iy,W)
      Call Sign(Mmon,Dday,Hhour,Year,Line,Count,Nn,Egim,2,Ysi,Szbil,Bby,
     &Ssy,Siy,Sign_Un,Iy,W)
      Call Ggap(Iy,Year,Mmon,Dday,Hhour,Line,Nn,Gap2)
      Call Ggap1(Iy,Year,Mmon,Dday,Hhour,Line,Nn,Bbz,Count,Egim,Gap3,
     &Evgap)
      Do 39 I=0,50
      Gap(Iy,I)=Gap2(I)
39    Continue
      Do 49 I=0,1
      Do 49 J=1,50
      GapA(Iy,I,J)=Gap3(I,J)
49    Continue
      Do 349 I=1,Nn
      Evngap(Iy,I)=Evgap(I)
349   Continue
!
!
      Write (Evn_Un,'(2I4)') Year,Nn
      Do 217 I=1,Nn
      Write (Evn_Un,'(11I4)') Ay(Iy,I),Gun(Iy,I),Saat(Iy,I),Line(Iy,I),
     &Egim(Iy,I),Szbil(Iy,I),Xsi(Iy,I),Ysi(Iy,I),Six(Iy,I),Siy(Iy,I),
     &Evngap(Iy,I)
217   Continue
!
!
333   Continue
      Do 83 I=0,50
      Write (Gap_Un,783) I,(Gap(J,I),J=1,20)
83    Continue
      Do 92 I=0,1
        If (I.eq.0) Then
           Write (Gap1_Un,*) 'Slope < 0'
        Else
           Write (Gap1_Un,*) 'Slope > 0'
        End If
      Do 92 J=1,50
      Write (Gap1_Un,783) J,(GapA(Iy,I,J),Iy=1,20)
92    Continue
783   Format (2x,I4,2x,20I4)
107   Format (4I2,4x,6F6.1)
      Stop
      End
!
! Subprogram for clock-counter control.
! If the two data do not belong to same day or month ,this subroutine
! carries a parameter (G1 <Integer> ) to main program to be able to
! the two data-times compared.
      Subroutine Date(M1,M2,D1,D2,Y,G1)
      Integer D1,D2,Y,G,G1,Div
      G=M2-M1
        If (G.eq.0) Then
           G1=D2-D1
        Else
```

```
            Div=Mod(Y+1900,4)
            Goto (1,2,1,3,1,3,1,1,3,1,3,1) M1
1           Max=31
            Goto 10
2           Max=29
            If (Div.gt.0) Max=28
            Goto 10
3           Max=30
10          G1=(Max-D1)+D2
         End If
      Return
      End
!
! Subprogram for event calculations.
      Subroutine Start(Bz1,Bza,Dt1,Slp,Nc)
      Integer Slp
      Sum1=Abs(Bz1+Bza)
      Sum2=Abs(Bz1)+Abs(Bza)
         If (Nint(Sum1).ne.Nint(Sum2)) Then
!
!    (!In this case there is an event !)
            Slope=(Bza-Bz1)/Dt1
            Slp=1
            If (Slope.lt.0.0) Slp=0
            Nc=2
         Else
            Nc=1
         End If
      Return
      End
!
! Sign distributions of Bx and By between t1-3hr and t2+3hr (t1 and t2
! are event times)
      Subroutine Sign (M,D,H,Year,Line,Count,Nn,Egim,Ij,Xy,Szbil,Bb,Ss
     &,Si,Sign Un,Iy,W)
      Real Bb(8500),Ss(8500)
      Integer M(8500),D(8500),H(8500),Year,Count,Sign Un,Xy(20,900)
      Integer T,G1,B(0:3),A(0:3),Egim(20,900),Szbil(20,900),W,Nn
      Integer Line(20,900),Si(20,900)
      Character*2 Sb(0:3),Ssb(900,0:3),Sa(0:3),Ssa(900,0:3),Sg*1
      Logical L1,L2,L3,L4
         If (Ij.eq.1) Then
            Do 13 I=1,Nn
            Si(Iy,I)=0
13          Xy(Iy,I)=4
         Else
            Do 51 I=1,Nn
            Si(Iy,I)=0
51          Xy(Iy,I)=44
         End If
      Do 80 I=1,Nn
      K=Line(Iy,I)
      Sb(1)='  '
      Sb(2)='  '
      Sb(3)='  '
      Do 90 J=1,3
      Igap=(K-1)-J
       If (Igap.gt.2) then
         Ih1=H(Igap)
         Ih2=H(K-1)
            If ((M(Igap).ne.M(K-1)).or.(D(Igap).ne.D(K-1))) Then
              Call Date (M(Igap),M(K-1),D(Igap),D(K-1),Year,G1)
              Ih2=Ih2+24*G1
            End If
         Idiff=Ih2-Ih1
            If (Idiff.le.3) Then
               Sb(Idiff)='+ '
               If (Bb(Igap).lt.0) Sb(Idiff)='- '
            End If
              If (I.gt.1) Then
                 If (I.eq.2) Then
```

```
                  It=I-1
               Else If (I.eq.3) Then
                  It=I-2
               Else
                  It=I-3
               End If
            Do 100 T=It,I
             If((Igap.eq.Line(Iy,T)).or.(Igap.eq.(Line(Iy,T)-1))) Then
!
! If the times at which we examine Bx and By signs match t1 or t2 time
! values which belong to other events,get +E or -E for SB(I) instead of
! + or -,respectively.
                If (Sb(Idiff).eq.'+ ') Then
                   Sb(Idiff)='+E'
                Else If (Sb(Idiff).eq.'- ') Then
                   Sb(Idiff)='-E'
                End If
              End If
100         Continue
            End If
         End If
90    Continue
      Ssb(I,1)=Sb(1)
      Ssb(I,2)=Sb(2)
      Ssb(I,3)=Sb(3)
80    Continue
      Do 180 I=1,Nn
      K=Line(Iy,I)
      Sa(1)='
      Sa(2)='  '
      Sa(3)='  '
      Do 190 J=1,3
      Igap=K+J
        If (Igap.lt.Count) Then
          Ih1=H(K)
          Ih2=H(Igap)
            If ((M(Igap).ne.M(K)).or.(D(Igap).ne.D(K))) Then
              Call Date (M(K),M(Igap),D(K),D(Igap),Year,G1)
              IH2=IH2+24*G1
            End If
          Idiff=Ih2-Ih1
            If (IDiff.Le.3) Then
              If (Bb(Igap).lt.0) Then
                 Sa(Idiff)='- '
              Else
                 Sa(Idiff)='+ '
              End If
            End If
               If (K.lt.Count) Then
            Do 200 T=I,I+3
             If((Igap.eq.Line(Iy,T)).or.(Igap.eq.(Line(Iy,T)-1))) Then
                   If (Sa(Idiff).eq.'+ ') Then
                      Sa(Idiff)='+E'
                   Else If (Sa(Idiff).eq.'- ') Then
                      Sa(Idiff)='-E'
                   End If
             End If
200         Continue
              End If
        End If
190   Continue
      Ssa(I,1)=Sa(1)
      Ssa(I,2)=Sa(2)
      Ssa(I,3)=Sa(3)
180   Continue
!
! Check the signs at t1 and t2
      Do 188 I=1,Nn
      K=Line(Iy,I)
```

```
      Ssb(I,0)='+ '
      Ssa(I,0)='+ '
      If (Bb(K-1).lt.0) Ssb(I,0)='- '
      If (Bb(K).lt.0) Ssa(I,0)='- '
188   Continue
!
! Cases in which there are no change in sign for Bx or By
      Do 207 I=1,Nn
      K=Line(IY,I)
      Do 215 J=0,3
      B(J)=2
      A(J)=2
         If ((Ssb(I,J).eq.'+E').or.(Ssb(I,J).eq.'+ ')) Then
            B(J)=1
         Else If ((Ssb(I,J).eq.'-E').or.(Ssb(I,J).eq.'- ')) Then
            B(J)=0
         End If
         If ((Ssa(I,J).eq.'+E').or.(Ssa(I,J).eq.'+ ')) Then
            A(J)=1
         Else If ((Ssa(I,J).eq.'-E').or.(Ssa(I,J).eq.'- ')) Then
            A(J)=0
         End If
215   Continue
        If (B(3).ne.2) Then
           L1=(B(3).eq.B(2)).and.(B(3).eq.B(1))
           L2=(B(3).eq.A(1)).and.(B(3).eq.A(2))
           L3=(B(3).eq.A(3)).or.(A(3).eq.2)
           L4=(B(3).eq.B(0)).and.(B(3).eq.A(0))
        If (L1.and.L2.and.L3.and.L4) Then
           If (Ij.eq.1) Then
              Xy(Iy,I)=1
           Else
              Xy(Iy,I)=11
           End If
           If (B(3).eq.0) Then
              Si(Iy,I)=2
           Else
              Si(Iy,I)=1
           End If
        End If
!--------------------------------------------------------------------------!
!                        Solar  Sector  Boundries                          !
!       There is no change in sign for Bx       until an event             !
!--------------------------------------------------------------------------!
      L2=B(1).ne.B(0)
                 If (L1.and.L2) Then
                    If (Ij.eq.1) Then
                       Xy(Iy,I)=2
                    Else
                       Xy(Iy,I)=22
                    End If
                    If (B(3).eq.0) Then
                       Si(Iy,I)=2
                    Else
                       Si(Iy,I)=1
                    End If
                 End If
           L1=(B(3).eq.B(2)).and.(B(3).eq.B(1))
           L2=(B(3).eq.B(0)).and.(B(3).ne.A(0))
           If (L1.and.L2) Then
              If (Ij.eq.1) Then
                 Xy(Iy,I)=3
              Else
                 Xy(Iy,I)=33
              End If
              If (B(3).eq.0) Then
                 Si(Iy,I)=2
              Else
                 Si(Iy,I)=1
              End If
           End If
```

```
          End If
207     Continue
        Return
        End
!
! In this subprogram, we determine whether there is a data gap between
! two consecutive events
        Subroutine Ggap(Iy,Year,Mmon,Dday,Hhour,Linb,Nn,Gap2)
        Integer Mmon(8500),Dday(8500),Linb(20,900),Year,Gap2(0:50)
        Integer Count,Nn,G1,Time,Gap(20,0:50),Gap1(20,0:50),Hhour(8500)
        Integer Line(900)
!
! Set GAP and GAP1 areas ---> zero
        Do 213 I=0,50
        Gap(Iy,I)=0
213     Gap1(Iy,I)=0

!
        Do 44 I=1,Nn
44      Line(I)=Linb(Iy,I)
        Do 50 I=0,50
        Gap2(I)=0
50      Continue
        Do 20 I=1,Nn-1
        Time=0
        J=Line(I)+1
25      Ihh1=Hhour(J-1)
        Ihh2=Hhour(J)
        If ((Mmon(J-1).ne.Mmon(J)).or.(Dday(J-1).ne.Dday(J))) Then
!
!
!
          G=(Mmon(J)-Mmon(J-1))
          If (G.eq.0) Then
             G1=Abs(Dday(J)-Dday(J-1))
          Else
             Div=Mod(Year+1900,4)
             Goto (1,2,1,3,1,3,1,1,3,1,3,1) Mmon(J-1)
1            Max=31
             Goto 10
2            Max=29
             If (Div.gt.0) Max=28
             Goto 10
3            Max=30
10           G1=(Max-Dday(J-1))+Dday(J)
          End If
!
!
!
            Ihh2=Ihh2+24*G1
        End If
            If (J.eq.Line(I+1)) Then
               K=Time
               If (Time.gt.50) K=50
               Gap(Iy,K)=Gap(Iy,K)+1
               Gap1(Iy,K)=Gap1(Iy,K)+1
               Goto 20
            End If
            If ((Ihh2-Ihh1).eq.1) Then
               Time=Time+1
               J=J+1
               Goto 25
            Else
               Gap(Iy,K)=Time
            End If
20      Continue
        Do 19 I=0,50
        Gap2(I)=Gap1(Iy,I)
19      Continue
        Return
        End
```

```
!
!     Here, We search how many times later Bz ,belonging to any event,
! changes its sign that of at t2.
      Subroutine Ggap1(Iy,Year,Mmon,Dday,Hhour,Linb,Nn,Bz,Cnt,Islp,Gap3,
     &Evgap)
      Real Bz(8500)
      Integer Mmon(8500),Dday(8500),Linb(20,900),Line(900),Year
      Integer Cnt,Nn,G1,Time,Gap3(0:1,50),Hhour(8500),Islp(20,900)
      Integer Evgap(900)
!
! Set GAP3 DATA ---> zero
      Do 213 I=0,1
      Do 213 J=1,50
      Gap3(I,J)=0
213   Continue
      Do 217 I=1,Nn
      Evgap(I)=999
217   Continue
!
      Do 44 I=1,Nn
      Line(I)=Linb(Iy,I)
44    Continue
      Do 20 I=1,Nn
      II=Islp(Iy,I)
      Time=0
      If (Line(I).lt.Cnt) Then
      Do 30 J=Line(I)+1,Cnt
      Ihh1=Hhour(J-1)
      Ihh2=Hhour(J)
      If ((Mmon(J-1).ne.Mmon(J)).or.(Dday(J-1).ne.Dday(J))) Then
!
!
!
        G=(Mmon(J)-Mmon(J-1))
        If (G.eq.0) Then
           G1=Abs(Dday(J)-Dday(J-1))
        Else
           Div=Mod(Year+1900,4)
           Goto (1,2,1,3,1,3,1,1,3,1,3,1) Mmon(J-1)
1          Max=31
           Goto 10
2          Max=29
           If (Div.gt.0) Max=28
           Goto 10
3          Max=30
10         G1=(Max-Dday(J-1))+Dday(J)
        End If
!
!
!
          Ihh2=Ihh2+24*G1
      End If
      Idiff=Ihh2-Ihh1
      If (Idiff.eq.1) Then
         If (Bz(J).lt.0) Then
            Isgn=0
         Else
            Isgn=1
         End If
      Time=Time+1
       If (Isgn.ne.II) Then
!      Else
          If (Time.gt.50) Time=50
          Gap3(II,Time)=Gap3(II,Time)+1
          Evgap(I)=Time
          Goto 20
       End If
      Else
         Goto 20
      End If
30    Continue
      End If
20    Continue
      Return
      End
```

CURRICULUM VITAE

Orhan GÖKÇÖL

- was born in ÇANKIRI, on the 10th September of 1968,
- was graduated from Üsküdar Örnek Lisesi in 1984,
- obtained his B.Sc. in Aeronautics at the İstanbul Teknik Üniversitesi Uçak ve Uzay Bilimleri Fakültesi, Uçak Mühendisliği Bölümü, in 1988,
- has been working as research assistant at the Space Science and Technology Department since July 1989.